PALAIOS
Emphasizing the impact of life on Earth's history

PALAIOS, 2024, v. 39, 301–322
Research Article
DOI: http://dx.doi.org/10.2110/palo.2024.009

THROUGH FIRE, AND THROUGH WATER, AN ABUNDANCE OF MID-DEVONIAN CHARCOAL

IAN J. GLASSPOOL[1,2] AND ROBERT A. GASTALDO[1,3]
[1]*Department of Geology, Colby College, Waterville Maine 04901 USA*
[2]*Field Museum of Natural History, Chicago Illinois 60605 USA*
[3]*Department of Paleobiology, NMNH Smithsonian Institution, Washington, DC, 20560, USA*
email: ian.glasspool@colby.edu

ABSTRACT: **Evidence of fire in the Middle Devonian remains globally scarce. Charcoalified mesofossils recovered from the Emsian–Eifelian Trout Valley and St. Froid Lake formations of Maine are direct evidence of wildfires proximal to the Acadian Orogen, formed as the Avalon terrane and the North American plate collided. These mesofossils include charred psilophytes, lycopsids, prototaxodioids, enigmatic taxa such as *Spongiophyton*, and coprolites. Here, fire combusted a senesced and partially decayed litter, and the intimately associated nematophytes, following a period of extended dryness. We envisage wildfires occurred during neap tide when exposure of the flora of this estuarine setting was prolonged. Herein we provide a reconstruction of this Middle Devonian landscape and its flora in which lightning generated by post-dry season storms ignited wildfires that propagated through an extensive psilophyte-dominated litter.**

INTRODUCTION

Wildfire is a natural phenomenon and fundamental Earth System process (Bond and Keeley 2005; Bowman et al. 2009; Pausas and Keeley 2009; Pausas et al. 2017) that has contributed to the shaping of the planet for at least the last 430 million years (Glasspool and Gastaldo 2022a). At present, fires burn on average around 3–5 million km^2 per year (Chuvieco et al. 2008; van der Werf et al. 2017). This level of combustion reduces plant-carbon storage by $\sim$ 10%, having profound impacts on both atmospheric composition and climate (Yue et al. 2016; van der Werf et al. 2017; Lasslop et al. 2019; Harrison et al. 2018, 2021; Jones et al. 2022). Wildfires impact the short-term Earth System through feedback on, amongst others, atmospheric concentrations of absorptive and reflective aerosols, and surface albedo through changes in vegetation cover. However, wildfire activity also feeds back into the long-term carbon cycle through the burial of organic matter (charcoal, soot), and its impact in promoting clastic sedimentation (see discussions in Bowman et al. 2009 and Scott 2010). The short-term outcome of the present fire-regime feedback on the Earth System is a 6 ppm rise in atmospheric levels of CO_2 for every 1°C of Mean Annual Temperature (MAT) rise (Harrison et al. 2018; Jones et al. 2022).

The fossil record of charcoal from the Silurian onwards, and hence wildfire, is largely continuous, with the Middle Devonian reported as a notable exception (Scott and Glasspool 2006). Devonian hothouse climate (Becker et al. 2020) fluctuated through this interval, exhibiting moderate swings of temperature between cooler and warmer, although it remained icecap free (Scotese et al. 2021). Macro- and mesofossil charcoal (hereafter simply charcoal) from the Middle Devonian remain largely undocumented. This paucity in the fossil record is more notable given that (1) global average temperatures (GAT) for the timeframe are calculated to have been at least 4.5°C warmer than the Present (Scotese et al. 2021), and (2) some biogeochemical box models, indicate this as a period of falling atmospheric oxygen concentration (e.g., Mills et al. 2023—however, note the important and circular feedback of the presence/absence of charcoal into models of deep time atmospheric oxygen concentration).

The cladoxylopsidalean order Pseudosporochnales are among some of the earliest arboreous plants and formed the first documented forests (Davies et al. 2024). The First Appearance Datum of these trees is in the Eifelian–Givetian (Stein et al. 2012, 2020). This plant order, including *Wattieza*/*Eospermatopteris* (Stein et al. 2007), was water dependent, fast-establishing and fast-growing, but not woody (Stein et al. 2012). Woody aneurophytaleans grew alongside these cladoxylopsids and tree-sized lycophytes at Gilboa Quarry in New York (Stein 2012). However, it was not until the advent of the archaeopteridaleans during the Givetian that the pseudosporochnaleans were joined by large, woody, deeply rooted and less water constrained trees (Beck 1962; Algeo et al. 2001; Stein et al. 2012). These plants provided an even more significant potential fuel source that would have been distributed through a greater and more seasonally drier diversity of habitats.

Middle Devonian, arboreous cladoxylopsids and archaeopterids have been extensively documented in recent years (e.g., Stein et al. 2007, 2012, 2020; Meyer-Berthaud et al. 2010; Decombeix et al. 2011; Giesen and Berry 2013; Marshall et al. 2022; Davies et al. 2024). However, other contemporaneous plant taxa were present on various landscapes (Berry and Fairon-Demaret 2001). This Middle Devonian (Eifelian–Givetian) flora included rhyniopsids (e.g., *Stockmansella*, Fairon-Demaret 1986), lycophytes (lycopsids [club mosses], zosterophylls, and barinophytes), basal euphyllophytes (the former trimerophytes; e.g., *Psilophyton* Dawson emend. Hueber and Banks 1967; *Pertica* Kasper and Andrews 1972; *Pauthecophyton* Xue et al. 2012; *Planatophyton* Gerrienne et al. 2014), monophilophytes (filicopsids [ferns], cladoxylopsids and sphenopsids [horsetails]), and lignophytes (progymnosperms). While embryophyte diversity decreased from the Emsian into the early-Middle Devonian it was once again expanding rapidly before the end of the Givetian (Berry and Fairon-Demaret 2001; Capel et al. 2022).

Middle Devonian terrestrial strata are not common in the USA, and Maine affords some of the best opportunities to study floras of this age. The Emsian–Eifelian Trout Valley Formation (TVFm) flora of Baxter State Park, Maine, was first reported by Dorf and Rankin (1962) and has been the subject of ongoing study since (Fig. 1; e.g., Dorf and Rankin 1962; Andrews et al. 1977; Kasper et al. 1988; Allen and Gastaldo 2006). The

Published Online: September 2024
 0883-1351/24/039-301

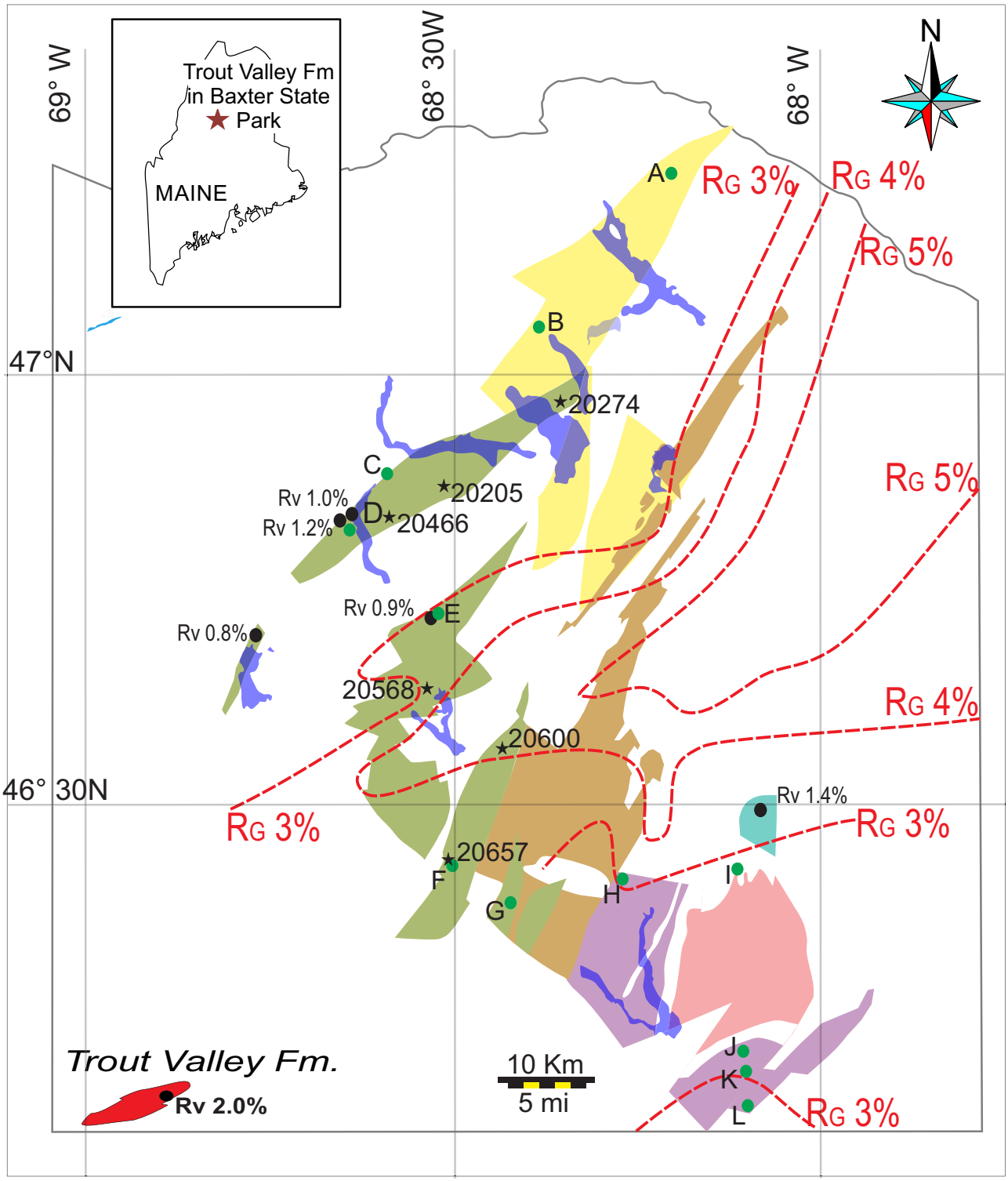

FIG. 1.—Map of northern Maine, USA, including overview of the State (inset) and the major regional lakes (dark blue), the location of the Emsian–Eifelian age Trout Valley Formation (red shaded), and the revised map of the distribution of Silurian to Devonian age marginal marine and terrestrial sediments in Aroostook County (Wang 2022). Color key: brown shading = Frenchville Formation (Silurian undifferentiated); pink shading = Chapman Formation (Pragian); yellow shading = St Agatha Formation (informal; Emsian); green shading = St. Froid Lake Formation (Emsian–Eifelian); purple = Scopan Lake Formation (informal; Pragian–Emsian); light blue shading = Mapleton Formation (Eifelian). Legend: dashed red lines (R_G %) = graptolite reflectance isograds extrapolated from Malinconico (1993a); black dots (R_V %) = Mean Random Vitrinite reflectance values calculated by Malinconico (2023); black, numbered stars are Wang collection localities from which samples have been macerated; green dots labeled A–L are Wang localities with palynological age data; A = Pragian–Emsian; B = Emsian; C = late Emsian; D = Lochkovian or younger; E = late Pragian to Middle Devonian; F = Emsian–Eifelian; G = late Pragian–Eifelian; H = late Pragian–Eifelian; I = late Pragian–early Emsian; J = Pragian–early Emsian; K = Pragian or younger; L = Pragian–early Emsian.

TABLE 1.—*Palynotaxa identified from the Trout Valley Formation (McGregor 1992).*

Palynomorphs	Comments
Acinosporites lindlarensis Riegel, 1968 var. *lindlarensis*	
?*Ancyrospora* sp.	Not reliably reported below uppermost Emsian
cf. *Apiculatasporites perpusillus* (Naumova) McGregor, 1973	
?*Apiculiretusispora plicata* (Allen) Streel, 1967	
Apiculiretusispora sp.	
Calamospora sp.	
cf. *Clivosispora verrucata* McGregor, 1973 var. *verrucata*	Questionable ID, range terminates in upper Emsian in E. North America/W. Europe
Deltoidospora sp. cf. *Q. priddyi* (Berry) McGregor, 1973	
?*Diatomozonotriletes oligodontus* Chibrikova, 1962	
?*Dibolisporites wetteldorfensis* Lanninger, 1968	Questionable ID, range terminates in upper Emsian in E. North America/W. Europe
Emphanisporites annulatus McGregor, 1961	
Emphanisporites rotatus McGregor, 1961	
Grandispora douglastownense McGregor, 1973	Not reliably reported below uppermost Emsian
Grandispora spp. (two species)	
Lophotriletes devonicus (Naumova ex Chibrikova) McGregor and Camfield, 1982	
Retusotriletes maculatus? McGregor and Camfield, 1976	Questionable ID, range terminates in upper Emsian in E. North America/W. Europe
Tholisporites sp. cf. *T. chulus* (Cramer) McGregor, 1973 var. *chulus*	
?*Verrucosisporites polygonalis* Lanninger, 1968	Questionable ID, range terminates in upper Emsian in E. North America/W. Europe
*Grandisporites velata**	
*Acinosporites acanthomammillatus**	

age of the TVFm is best constrained palynologically, despite the highly coalified nature of the palynoflora (Thermal Alteration Index 4-[$\sim R_o v$ 1.5 to 2.0] to 4 [$R_o v > 2.0$]; McGregor 1992; for correlation with $R_o v$ see Mastalerz et al. 2016). Both Richardson and McGregor (1986) and McGregor (1992) concluded that the flora lies between the latest Emsian and very early Eifelian. The palynomorphs (Table 1) are assignable to the *Grandispora douglastownense-Ancyrospora eurypterota* spore Assemblage Zone, which spans the Lower/Middle Devonian boundary (Richardson and McGregor 1986). This zonation would correlate with the *Polygnathus patulus-costatus* conodont zones (late Emsian–early Eifelian) or possibly the *P. partitus-costatus* zones (early Eifelian; McGregor 1992) of Western Europe.

The age assignment of the TVFm is taphonomically dependent (McGregor 1992). If the Emsian-age taxa are recovered from *in situ* (autochthonous) deposits, a correlation with the upper Wetteldorf or the lower Reisdorf Formations of the Eifel region, Germany, indicate a very late Emsian age. Such an age would not be discrepant with the presence of *G. douglastownense* and ancyrate megaspores, as their lowest biostratigraphic range extends into the very late Emsian in eastern Canada (McGregor and Camfield 1976; McGregor 1977, 1992). However, if the Emsian palynotaxa were recycled into younger-aged sediments, the TVFm could be as young as early Eifelian. This age would be in accord with the presence of ?*Diatomozonotriletes oligodontus* and as young as *Lophotriletes devonicus*; neither taxon is known to predate the Eifelian in North America or Western Europe. We note, though, that these ranges may be skewed by their infrequent documentation.

The two most frequently encountered megafloral components of the TVFm flora are *Pertica quadrifaria* and *Psilophyton* spp., which are intermixed with other taxa. Herein, we examine taphonomically enigmatic mesofossils obtained from the TVFm by acid maceration and report on their diversity, nature, and preservation. In addition, recent mapping of northern Maine in Aroostook County (Fig. 1; Wang 2022) has afforded an opportunity to collect, process, and evaluate roughly contemporaneous material, which is complementary to the Trout Valley flora.

SETTING

At a latitude at most 30°S of the equator (Scotese and McKerrow 1990) the terrestrial TVFm strata accumulated as part of a thick clastic foreland-basin succession (Bradley et al. 2000; Allen and Gastaldo 2006). These were deposited to the northwest of the Acadian orogeny, as the Avalon terrane and the North American plate collided (Gastaldo 2016). During collision a volcanic island chain was located to the east of the land mass, with this subsequently welded with the continent. The Traveler Mountain Rhyolite (406–407 Ma) is interpreted as volcanic flows from the caldera of one of these volcanoes (Bradley and Tucker 2002). Erosion, weathering, transport, and proximal deposition of these volcanics resulted in the deposition of the TVFm to the northwest of the Acadian highlands.

The formation itself comprises pebble conglomerate, fluvial and near-shore sandstone, and siltstone of muddy tidal flats. Paleosols developed next to estuarine-influence rivers transporting coarse-and-fine clastic sediments to a coastline under brackish water influence (Selover et al. 2005; Allen and Gastaldo 2006), and the subtropical climate exhibited pronounced wet to dry seasonality (Allen and Gastaldo 2006). Most of the recorded flora was transported and deposited as drapes on bedding surfaces, although very fine rootlets in the mudflats indicate its colonization (for details of the sedimentology see Allen and Gastaldo 2006; Gastaldo 2016).

Dorf and Rankin (1962) first recognized the fossiliferous nature of these strata reporting both plant-and-invertebrate fossils including psilophytes, eurypterids, ostracods, bivalves, and estherids in rocks exposed along Trout Brook. The flora is reported from a variety of sedimentary settings throughout the TVFm and is summarized in Table 2 (updated from Allen and Gastaldo 2006). Palynology indicates these strata, which rest unconformably on the Traveler Rhyolite, are of latest Emsian to earliest Eifelian age (McGregor 1992), an age corroborated by the macroflora (Kasper et al. 1988). To date, all fossils originate from rock exposed either along Trout Brook, its tributaries (South Branch Ponds Brook and Dry Brook), or as pavement outcropping on the Wadleigh Mountain Road running parallel to, and just to the north of the Trout Brook (Fig. 2; Gastaldo 2016).

Comparable in age with the TVFm, and paleogeographically proximal, is the newly named St. Froid Lake Fm. (Fig. 1; Wang 2022). Until recently, the terrestrial or near-shore Silurian and Devonian floras of northern Maine (Table 3) comprised those from the Frenchville (Silurian), the Fish River Lake Fm. (late Silurian–late Eifelian), the Chapman Fm. (Lochkovian–Pragian), and the Eifelian-age Mapleton Fm. (Bradley et al. 2000; Bradley and Tucker 2002). The pre-Acadian, fault-bounded St.

TABLE 2.—*Floral distribution in Trout Valley Formation facies (updated from Allen and Gastaldo 2006).*

Fluvial		Estuarine		
Braided fluvial or alluvial fan	Migrating braided channels	Flood basin/Overbank	Incipient wetland soil	Estuarine/Tidal flats and channels
Prototaxites sp. *Taeniocrada* sp	*Taeniocradia* sp. *Drepanophycus* sp. *D. gaspianus* *Leclercqia complexa* *Pertica quadrifaria* *Psilophyton* sp. *P. dapsile* *P. forbesii* *P. princeps*	*Leclercqia* sp. *Pertica quadrifaria* *Psilophyton* sp. *P. forbesii*	*Psilophyton* sp. *P. forbesii*	*Sciadophyton* sp. *Sporognites* sp. *Taeniocrada* sp. *Drepanophycus gaspianus* *Kaulingophyton* sp. *K. akantha* *Leclercqia* sp. *L. complexa* *Pertica quadrifaria* *Psilophyton* sp. *P. dapsile* *P. forbesii* *P. microspinosum*

Froid Lake Fm. accumulated in a shallow, near-shore, low energy environment. The sediments comprise non-foliated, multi-hued, thin sandy and coaly beds of comminuted dark phytoclasts (Gastaldo 1994). These are interbedded with medium-thin, tabular, reddish-brown or buff, ripple cross-laminated sandstone. The deposits are similar to those described from the Fish River chain of lakes and the Ashland area (Wang et al. 2020). The formation also contains thin (< 3 cm) shaley-siltstone and dark shale interbedded with phytoclast drapes. Bioturbation is recorded very locally and the fauna consists of brachiopods including *Leptocoelia flabellites*, *Beachia*, *Atlanticocoelia*, *Acrospirifer*, and *Hysteriolites* spp. These invertebrates indicate an Emsian age for the unit (Wang 2022). The floral phytodebris comprises abundant transported and comminuted

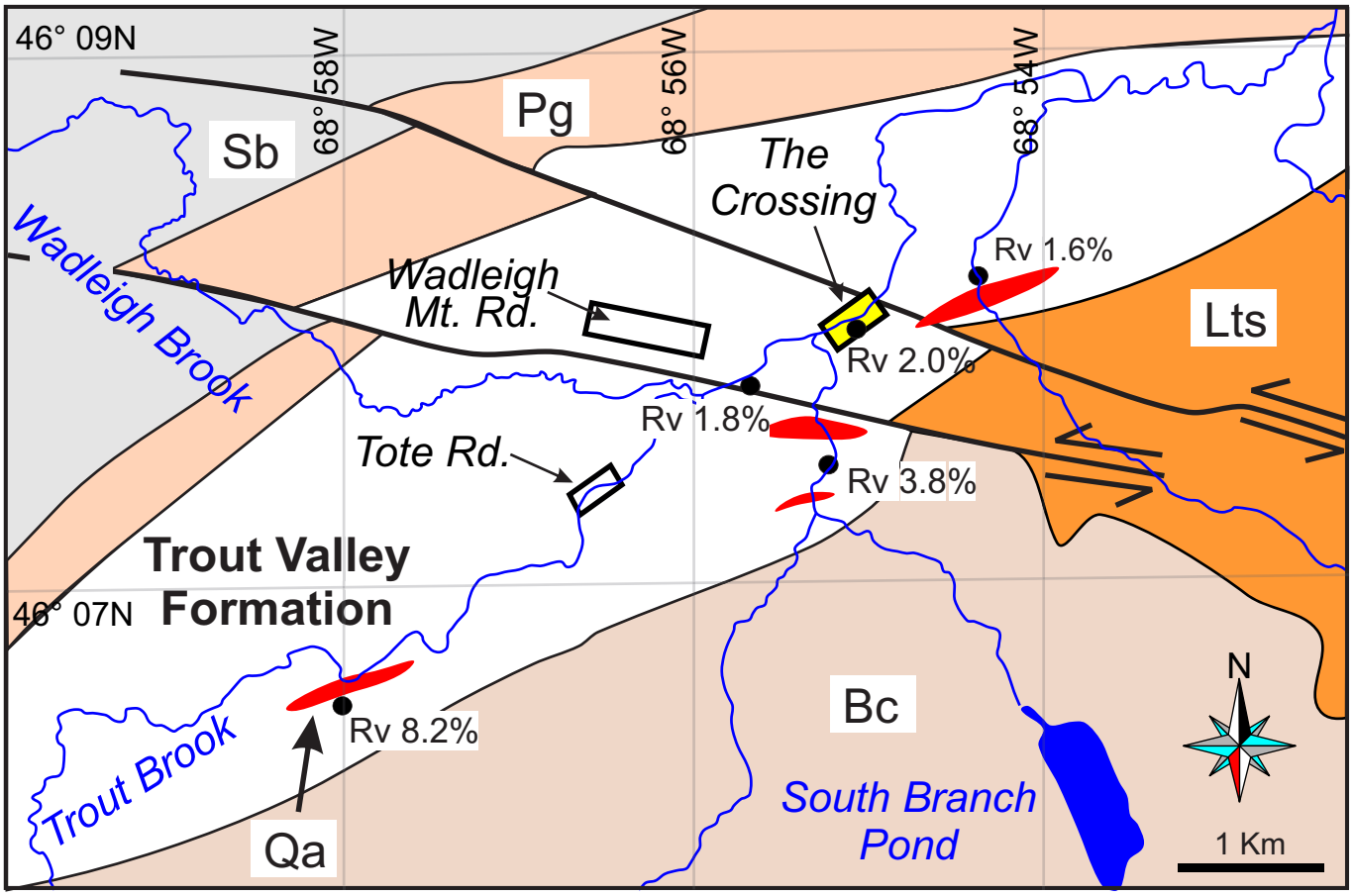

FIG. 2.—Bedrock geological map of the northern region of Baxter State Park, Maine, USA. Emsian–Eifelian age Trout Valley Formation (white area); Bc = Black Cat Member of the Traveler Rhyolite; Lts = Late stage lavas and tuffs; Pg = Pogy Member of the Traveler Rhyolite; Qa = quartz andesite intrusions; Sb = Seboomook Group. Boxed areas are those from which samples were collected for this study. Black dots (R_V %) are Mean Random Vitrinite reflectance values (Rv) calculated by Malinconico (2023).

TABLE 3.—*The floral components of the Silurian to Devonian of northern Maine as compiled from prior publications. There is considerable doubt that* Eohostimella heathana *(Schopf et al. 1966) was a plant, let alone a land plant (Strother and Lenk 1983; Edwards et al. 2015). The flora from the Chapman Formation at Edmunds Hill (46°39′11″N 68°06′34″W), defined by its marine fauna, comprises just a few specimens of the enigmatic fossil* Pachytheca *(Schopf 1964). The diachronous Fish River Lake Formation has now been remapped and incorporates in part the SFLFm (Wang 2022). Taxonomic identifications after: (1) Schopf et al. 1966; (2) Kasper et al. 1974; (3) Kasper and Forbes 1983; (4) Schopf 1964; (5) Andrews and Kasper 1970; (6) Allen and Gastaldo 2006; (7) Andrews et al. 1977; (8) Gensel et al. 1969; (9) Dorf and Rankin 1962; (10) Kasper and Andrews 1972; (11) Andrews et al. 1968; (12) Kasper et al. 1988.*

Formation	Age	Identified floral components	
Mapleton Fm.	Eifelian	cf. *Stolbergia* sp. (12)	Lycophytes
		Barrandeina (?) *aroostookensis* (4)	?Cladoxylopsid
		Calamophyton forbseii (4)	Cladoxylopsid
		cf. *Calamophyton* sp. (12)	Cladoxylopsid
		cf. *Caladophyton* sp. (12)	Cladoxylopsid
		cf. *Schizopodium sp.* (12)	Cladoxylopsid
		cf. *Rhachophyton* sp. (12)	Aneurophyte
		Aphyllopteris sp. (4)	*Insertae sedis*
		Hostinella sp. (4)	*Insertae sedis*
Trout Valley Fm.	Emsian–Eifelian	*Prototaxites* sp. (5)	Nematophyte
		Sciadophyton sp. (6)	Rhyniophyte
		Sprogonites sp. (6)	Bryophyte
		Taeniocrada sp. (5)	Rhyniophyte
		Drepanophycus sp. (7)	Lycopsid
		Kaulaniophyton akantha (8)	Lycopsid
		Leclercqia complexa (6)	Lycopsid
		Sawdonia ornata (9)	Lycophyte
		Pertica quadrifaria (10)	Basal euphyllophyte
		Psilophyton dapisile (2)	Basal euphyllophyte
		Psolphyton forbseii (11)	Basal euphyllophyte
		Psilophyton microspinsosum (2)	Basal euphyllophyte
		Psilophyton princeps (2)	Basal euphyllophyte
		Thursophyton s sp. (7)	*Insertae sedis*
Chapman Sandstone	Pragian	*Pachytheca* sp. (4)	*Incertae sedis*
Fish River Lake Fm.	late Silurian–late Eifelian	cf. *Dawsonites arcuatus* (cf. *Psilophyton acuatum*) (2)	Basal Euphyllophyte
		cf. *Psilophyton dapsile* (3)	Basal Euphyllophyte
Frenchville Fm.	Silurian	*Eohostimella heathana* (1)	*Incertae sedis*

terrestrial plant fossils, probably trimerophytes (e.g., *Psilophyton* and *Pertica*) and *Hostinella* (Boone 1970), and larger centimeter-sized specimens of cf. *Protolepidodendron* sp. (Wang personal communication 2020). Environmentally, Wang (2022) compares the formation with both the contemporaneous Campbellton Fm. of northern New Brunswick (Kennedy et al. 2012) and the TVFm in Baxter State Park, Maine (Allen et al. 2006; Gastaldo 2016).

Areas of the Fish River Lake Fm., previously considered late Silurian in age (Bradley et al. 2000, table 1), have been remapped and assigned to the earliest Devonian marine Seboomook Group. Fossil plants from the Emsian–Eifelian age (Charles Wellman personal communication 2023, based on palynology) St. Froid Lake Fm. (SFLFm) are dominated by basal euphyllophytes (psilophytes; Kasper et al. 1974). These assemblages are similar to the contemporaneous TVFm, which is dominated by basal euphyllophytes and lycophytes. In contrast, the slightly younger Mapleton Fm. flora is dominated by cladoxylopsids with subsidiary progymnosperms (cf. *Rhacophyton* sp.) and lycophytes.

Mapping of Aroostook County, Maine, by Wang et al. (2020) and Wang (2022) is ongoing and he has recognized a far greater suite of terrestrial Devonian sediments in the region than had been previously conceived (Fig. 1). These fault-defined units include the informally named "Scopan Lake formation". The formation comprises a series of green-and-red sandstones with minor shale, thin felsic volcanics, and beds of fragmentary phytoclasts. The palynostratigraphic age of this informal unit is Pragian–Emsian (Charles Wellman personal communication 2023), although Wang considers a Pragian age to be more likely (personal communication 2023).

MATERIALS AND METHODS

Samples from Baxter State Park were collected over multiple years during Park-sanctioned Colby College collecting trips (see Gastaldo 2016; Allen and Gastaldo 2004; Selover et al. 2005). Unauthorized collecting in the Baxter State Park is strictly prohibited. All study materials will be curated at the Maine State Museum, Augusta, and remain sole property of the Baxter State Park Authority.

The TVFm is located in the NW part of Baxter State Park, northern Maine, located in T6 R9, T5 R9, and T5 R10 (Frost Pond and Wassataquoik, Maine, USGS 7.5′ quadrangles; Fig. 2). Outcrops occur along the Trout Brook and include the localities of Dorf and Rankin (1962), Andrews et al. (1977), and Allen and Gastaldo (2006). Outcrops exposed along Trout Brook (N46.13556°, W-68.91554°) and South Branch Ponds Brook (N46.12135°, W-68.92217°) are small, all $<$ 100 m in length and $<$ 7.1 m in height, and dip to the NW at 15° (Bradley et al. 2000). Samples were also collected from a 1.1 km stretch along the Wadleigh Mountain Road (N46.13383°, W-068.94905°; Fig. 2) beginning near where Lynx Road joins the roadway in the Scientific Forest Management Area and heading westward (Gastaldo 2016). Samples from across these localities were macerated but did not yield more than charred fragmentary unidentifiable detritus. However, "The Crossing" locality (N46.13568°, W-068.91571°) paleosol horizon yielded abundant charred and uncharred fossil plant material and forms the basis for the current study.

During mapping of the St. Froid Lake Fm., Aroostook County, Maine, Chunzeng Wang provided samples of intervals in which phytoclasts were

encountered. Macerated samples include: a red-brown sandstone of the "Red River redbeds basin" (Wang sample # 20205; N47.00111°, W-068.51944°) in which cf. *Protolepidodendron* sp. was reported on 11 Jul 2020 at this locality; a green sandstone-mudstone from the "Square Lake greenbeds" (20274; N47.08667°, W-068.34917°); a green sandstone-mudstone from the "Burpee Brook valley greenbeds basin" (20646; N46.97333°, W-068.57611°); a green sandstone-mudstone of the "Portage Lake greenbeds basin" (20568; N46.81444°, W-068.53861°); and green sandstone-mudstone samples (20600; N46.76278°, W-068.43556°; and 20657 N46.65750°, W-068.50250°) from the "Burpee Brook valley greenbeds basin." Samples also originated from: the Pragian-age Chapman Formation at Dragon Products, Edmunds Hill Quarry, 512 Carvell Road, Chapman, ME (N46.65306°, W-068.10944°; see Schopf 1964); and the early-middle Eifelian *Grandispora velatus-Rhabdospora langii* biozone within the Upper Member of the Mapleton Formation at Winslow Farm (N46.69586°, W-068.07818°; see Schopf 1964; Kasper et al. 1988). Macerations of Frenchville Fm. samples came from: Stockholm (N47.07333°, W-068.14722°; see Schopf et al. 1966); the Seboomook Fm. at Eagle Lake (N47.01667°, W-068.59139°) close to McGregor stations 95MDw116A and 95MDw117 (Bradley et al. 2000); and the Fish River Lake Fm. (N46.96157°, W-068.66979°) close to McGregor station CL-186 (Bradley et al. 2000).

Organic-rich samples (30 gm each from the St. Froid Lake Fm. and the TVFm., Wadleigh Brook Road; bulk [kilograms] quantities of the TVFm "The Crossing" locality) were first macerated using standard techniques for mesofossils (Pearson and Scott 1999), being treated with 37% HCl, followed by 30–40% HF, and subsequent treatment with hot HCL to remove fluorides. Residues were sieved to 150 μm and then picked both wet and dry under a Zeiss dissecting microscope at variable magnifications. Specimens overtly representing tissues and organs were picked first and preferentially, but subsequent selection was undertaken to randomly sample the macerates. Multiple specimens were mounted onto a single SEM stub with 12 mm Pelco adhesive tabs. A pie-shaped wedged notch cut out of each tab acts as an landmark when viewing by SEM, a reference point for numbering mounted specimens (first number is immediately to the right of the notch at the periphery of the stub with subsequent specimens being numbered clockwise around its periphery to the left hand side of the notch), and a marker for each photograph taken as an overview of the collection. When possible, additional specimens were positioned in concentric circles within the outer shell of samples, with numbering following the same logical order. Once mounted, specimens were gold coated (~ 90 s) using an SPI-Module sputter coater and analyzed with an Hitachi S-2700 scanning electron microscope.

Selected specimens were removed from the stubs after imaging and transferred to resin molds for embedding. Where specimens were millimetric in scale they were first set in silicon rubber square-tipped TEM molds and embedded in a low-viscosity epoxy resin (Struers Epofix) following ISO 7404-2 2009 standards. These specimens were carefully oriented prior to resin hardening. Then, each block was re-embedded in Epofix in a larger mold for grinding and polishing once hardened. In addition to the taxonomically significant material that followed this preparation pathway, a random selection of the remaining organic material was concentrated and embedded as a strew mount without prior electron microscopy and orientation. The aim of these strews was to provide an unbiased sampling of the material to explore the range of their physical properties in reflected light. Epoxy blocks with the SEM-and-strew specimens were ground with a sequential series of abrasive papers, ranging from 120 to 5000 grit. A penultimate polish on woven cloth was dosed with 1 μm polycrystalline diamond suspension. Final polishing was done on a napped cloth with a 0.05 μm aluminum-oxide slurry.

Quantitative measurements (mean random reflectance [MRR] in oil, Ro %) were made using a Leica DMR microscope fitted with a 50× oil immersion objective. Observations adhere to standard techniques (ISO 7404-5 1994); an Infinity 1 digital camera with Infinity Capture software was used for image acquisition. Calibration of the system and its linearity was conducted using at least four mineral standards closest in reflectance value to the material being measured. Standards used ranged from spinel (Ro = 0.42%) to silicon carbide (Ro = 7.93%). An oil blank was used, where necessary, to calibrate extremely low reflecting material. Where feasible, each specimen was measured at 100 points. However, the small scale of some specimens precluded meaningful counts of this size because of edge effects and imperfections of the polish; in these cases, as many points were counted as was practicable.

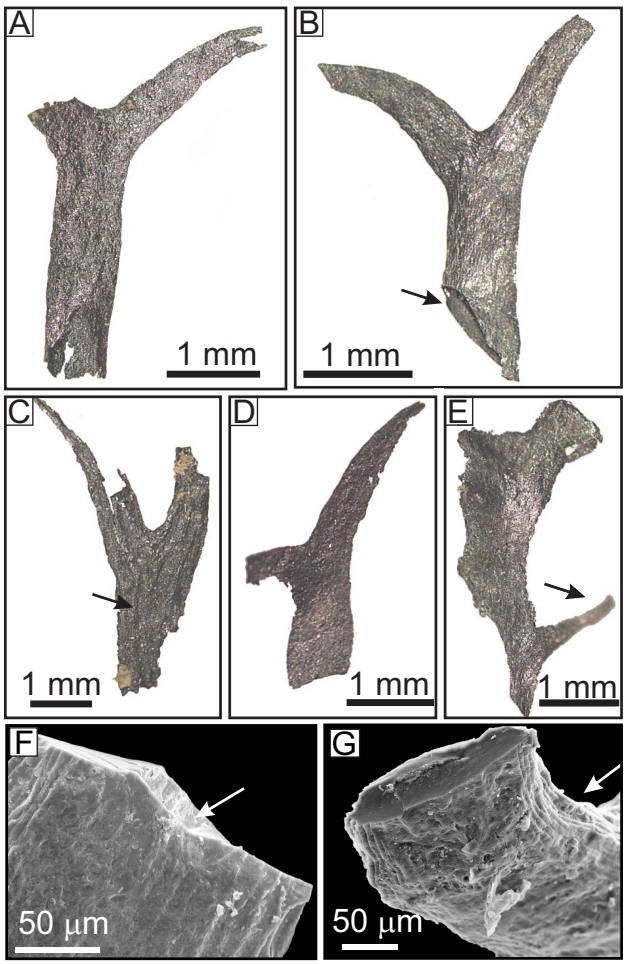

FIG. 3.—Psilophyte preservation in Trout Valley Formation paleosol at "The Crossing" (Fig. 2). Image acquisition, incident light (A–E), SEM (F, G). **A**) Psilophyte, black, lustrous, 3D incompletely preserved bifid terminal appendage (P-S3-S3). **B**) cf. *Pertica quadrifaria*, black, lustrous, 3D preserved bifid terminal appendage, arrow indicates vitreous fracture and gelified interior (P-S3-S2). **C**) cf. *Psilophyton forbesii*, black, lustrous, 3D incompletely preserved bifid terminal appendage with strong ribbing (arrow) and an acute angle-appendage divergence (P-S2-S1). **D**) Psilophyte, a compressed, lusterless bifid terminal appendage lacking cellular preservation (P-S6-S11). **E**) cf. *Psilophyton microspinosum* a short stem fragment below a dichotomy, with a spine (arrow) (P-S2-S3). **F**) Detail of Fig. 3B (P-S3-S2), right hand appendage apex confirming the lack of internal anatomy and vitreous fracture (arrow). **G**) Psilophyte, detailed image of an incomplete terminal appendage showing homogenous, vitreous internal preservation, but with the impression of original cuticular ribbing discernible (arrow; P-S4-S6).

Bireflectance data were gathered in plane-polarized light at 546 nm wavelength with a 50× oil immersion lens (ISO 7404-5 1994). The stage was rotated by 18° through the full 360° rotation possible and the reflectance was measured on the same pixel of the specimen at each 18° interval. Images were calibrated against the same standards as used for the MRR. A 22° Smith reflector cube was used to measure the degree of rotation of plane polarized light (see Gribble and Hall 1992). The use of the Smith reflector

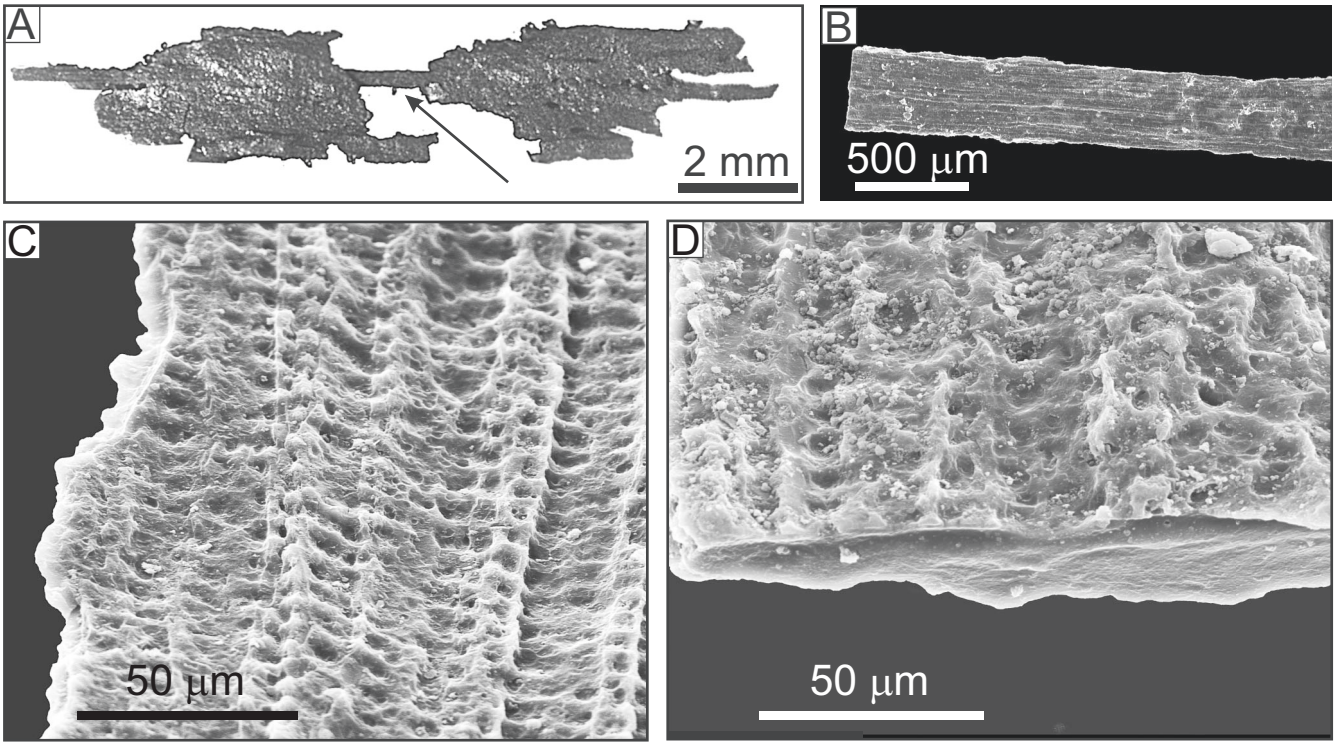

FIG. 4.—Non-charred psilophyte vascular tissues from the "The Crossing" (Fig. 2). Image acquisition: A) incident light; B–D) SEM. **A**) Compressed psilophyte axis, with preserved vascular strand (arrow; 2021-S1-S2). **B**) Compressed, isolated psilophyte vascular strand (2021-S6-S3). **C**) Detail of B showing impressions of scalariform vascular tissues typical of *Psilophyton.* **D**) Detail of B showing vitreous homogenization of the vascular strand.

cube results in a lower efficiency than the 45° BF reflector cube, but extinction with the former is uniform in an isotropic field unlike with the latter. Each specimen was leveled using a press and once mounted on a rotating polarized microscope stage, was checked to assess the accuracy of its leveling through examination of an isotropic standard (see Crelling et al. 2005). Isotropic standards that are not leveled accurately appear to show weak bireflectance, not detectable by the eye, but resulting from a slight inclination of the specimen. Inaccurate leveling is expressed in the reflectance sine wave following rotation of the specimen through 360°, where the data will conform to a sine wave with a single minimum versus the two-extinction minima that would be expected as a result of rotation of a leveled isotropic specimen. Unknown specimens were assessed for the accuracy of press leveling by removing the objective lens from the light path and stopping the field diaphragm down. This permits an image of the field diaphragm to become discernible on the specimen and enables any further required leveling to be carried out by manual adjustment of the block until, on rotation, no movement of the diaphragm image was discernible. Bireflectance data ($R_{max} - R_{min[apparent]}$) were measured from the reflectance data gathered per-site of measurement through 360° of stage rotation.

RESULTS

A variety of psilophyte organs were recovered from "The Crossing" paleosol horizon where preservation was varied. Superficially, most organs appear charred (Fig. 3A–3E). These are black, showing a high luster, some degree of 3D relief and, when viewed in incident light using a dissecting microscope, appear to preserve cellular level details. While black in coloration, several specimens appear compressed, lusterless, and lack cellular level details (i.e., Fig. 3D). Closer examination of charred specimens reveals several taphonomic differences in the material. For example, one specimen (Fig. 3B) preserves no internal anatomy, but internally is homogenous, solid, and breaks with a vitreous fracture (Fig. 3F, arrow). Other organs superficially show anatomical preservation, including scalariform thickenings (e.g., Figs. 3G, arrow, 4A–4D), but have no internal anatomy, appearing gelified. This atypical preservation exhibits compression while maintaining a discreetly fossilized vascular strand with anatomical level impression data (Fig. 4A–4D).

Hooked Terminal Appendages

The incomplete nature, small size, and variable features of the plant organ-hook morphotypes complicates identification. For example, the absence of a second hooked appendage (Fig. 3A) eliminates the opportunity to confidently assess the angle between them, which Kasper et al. (1974) used to differentiate taxa. This incomplete specimen is similar to both *Pertica quadrifaria* and *Psilophyton microspinosum* (Kasper and Andrews 1972; Kasper et al. 1974). In other cases, specimens most closely resemble *P. quadrifaria* (Fig. 3B) or *Psilophyton forbesii* (Fig. 3C; see Andrews et al. 1968, fig. 10), the latter of which has a strongly ribbed surface and an acute angle between the terminal appendages (Kasper et al. 1974, fig. 41). Several specimens should, at best, be termed a psilophyte (Fig. 3D, 3E; basal euphyllophyte). We interpret Figure 3E to represent a small stem fragment below a dichotomy, with the arrowed feature representing a spine, which measures 0.4 m in width at its emergence from the stem measure and tapers along its 1.1 mm in length, abruptly terminating. We tentatively assign this form to *Psilophyton microspinosum*, although the spine is half its reported length (Kasper et al. 1974).

The most abundant hooked appendage morphotype (Fig. 5A–5F) is a small (< 3 mm tall $\times$ 3 mm tip-to-tip wide, pre-bifurcate axis < 1 mm in width) recurved organ, closely resembling those of *Pertica quadrifaria* (Andrews and

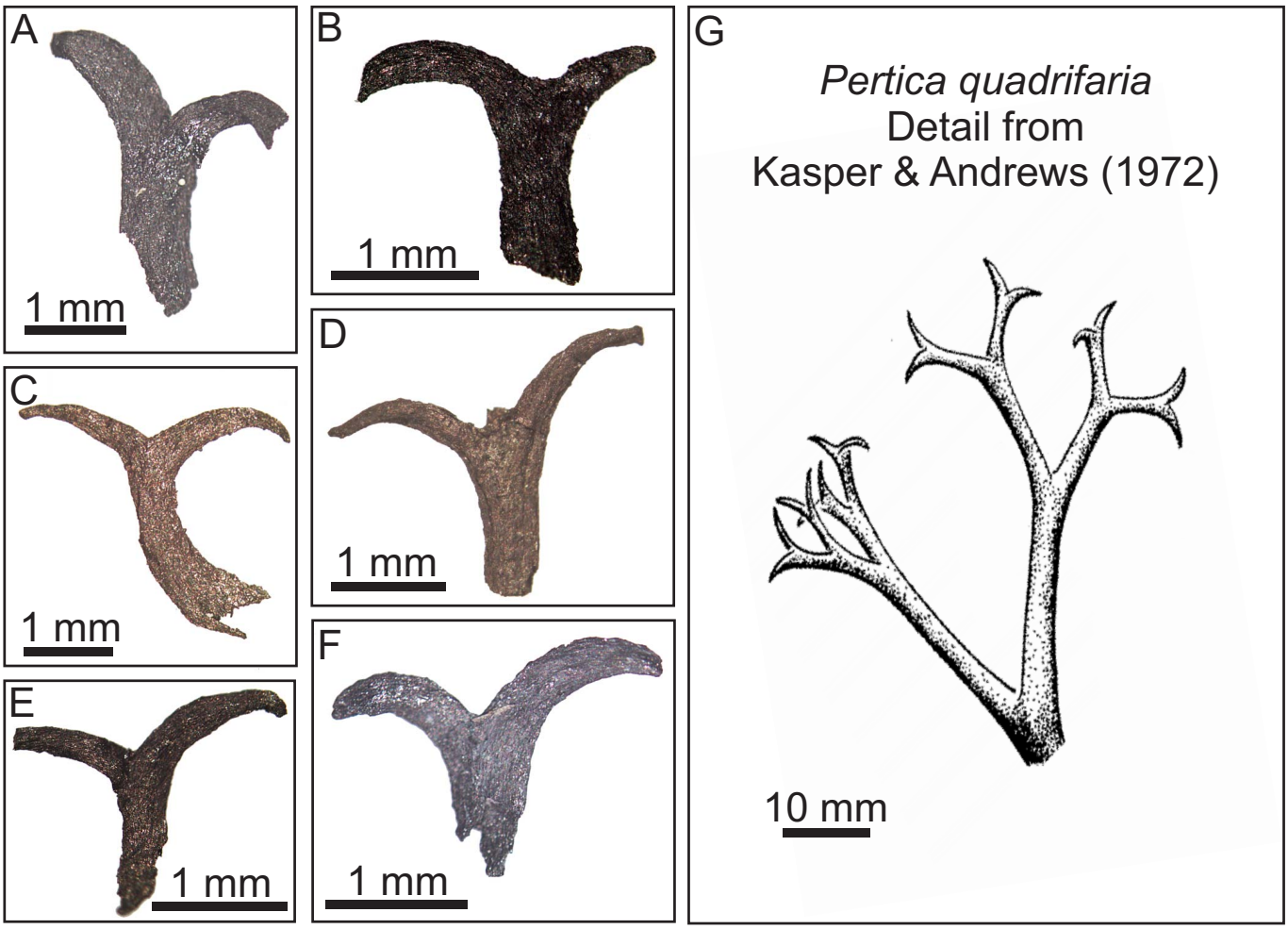

FIG. 5.—Trout Valley specimens in incident light. **A–F**) Charred, 3D preserved, terminal psilophyte appendages. cf. *Pertica quadrifaria.* Samples: A, P-S6-S4; B, P-S4-S14; C, P-S6-S1; D, P-S6-S13; E, P-S4-S10; F, P-S6-S2. **G**) Detail from Kasper and Andrews (1972, fig. 10) *Pertica quadrifaria* reconstruction.

Kasper 1972). However, once viewed at higher SEM magnification (Figs. 6, 7), there are discernible differences amongst these organs. Most hooked processes terminate at a single apex. However, some (n = 2) bifurcate distally in the last 150–200 μm at their very apex (Fig. 7A–7D) and are bluntly rounded with no obvious secretory or acute spinose features (Fig. 7B–7D). While superficially well-preserved, even at low magnification viewed by SEM (Fig. 6A), most specimens show decay features (Fig. 6D, 6F, 6G). For example, the specimen illustrated in Figure 6 clearly underwent decay although it exhibits unlaminated (homogenous) cell walls (Fig. 6C, arrow) that are indicative of charring. Compressed specimens (Fig. 6D) show little evidence of internal anatomy although spine apices are clearly preserved (Fig. 6C). Sporadic evidence of original plant cuticle is present in some specimens (e.g., Fig. 6D), although it has been lost or damaged in most instances (Fig. 6E–6G). There is limited evidence of tissue blistering (Fig. 6E; see Edwards and Axe 2004) which, again, is indicative of the effects of charring. Signs of fungal/nematophytic activity are also present with larger (Fig. 6F, arrow) and smaller tubes welded and adhered to the appendage (Fig. 6G, arrow).

Other Terminal Appendage Morphotypes

Three additional terminal psilophyte-appendage morphologies are in the TVFm material. The first (Fig. 8A, 8B) comprises more robust enations (n = 2) wherein the axis is up to 1 mm in width prior to dichotomizing. Their apices dichotomize at an angle 90°, producing rigid spines from 0.5 to ~ 1 mm long and most closely resemble the sterile termini illustrated by Kasper et al. (1974, fig. 10) of *Psilophyton dapsile*. However, this material was originally described with a maximum stem width of 2 mm with "*ultimate branchlet*(s) *with a diameter of less than 1 mm*" and *"closely dichotomizing ultimate branchlets.*" Their description is based solely on the fertile branches while not describing the sterile units. SEM of the most distal apex (Fig. 8C) in the TVFm material shows a pore-like opening.

The second and third appendage morphotypes differ (Figs. 9, 10). The second (Fig. 9A–9D) demonstrates a final dichotomy at an angle of 105° (± 1–2°). This feature, while not part of the systematic diagnosis, was detailed in *Psilophyton microspinosum* (Kasper et al. 1974). The ultimate divisions (Fig. 9A–9D) of incomplete appendages measure 3, 4, 1, and 2 mm, respectively, and are shorter than the 5 mm described by Kasper et al. (1974; with the possible exception of Fig. 9A). Similarly, the limb giving rise to these divisions may be long (Fig. 9D = 5.5 mm), although short of the 1.6 cm reported by the authors. The third appendage morphotype (Fig. 10A–10C) is united by the presence of strong ribbing and an acute dichotomous angle, in which some terminal processes are curved inwards. These are comparable with illustrations of *Psilophyton forbesii* (Andrews et al. 1968, Fig. 10).

All sporangial remains are psilophyte in overall morphology (Fig. 11A–11I) and fall into two size categories; those 4.5 mm in length (Fig. 11A,

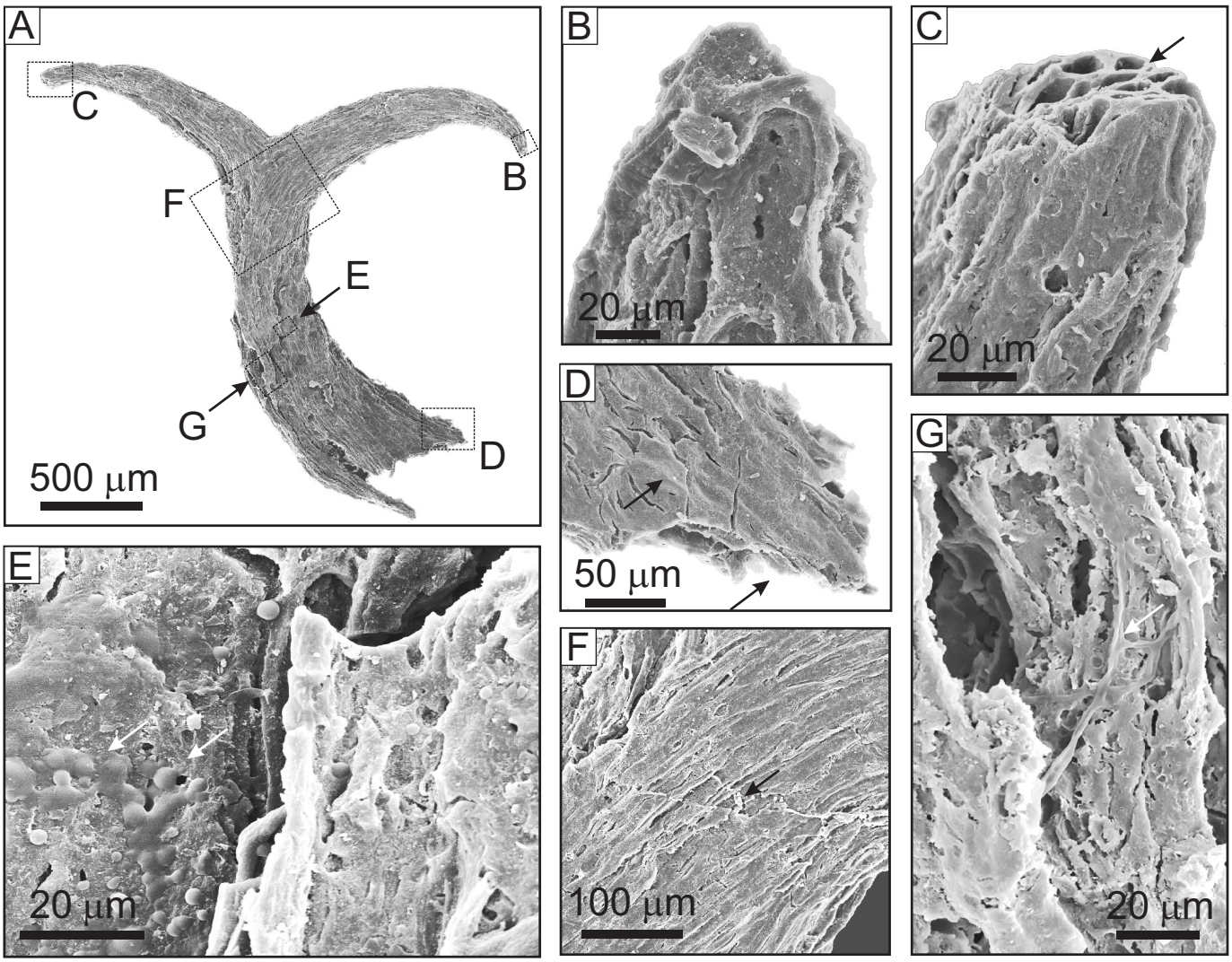

FIG. 6.—Trout Valley SEM images of P-S6-S1 (Fig. 5C). **A**) Overview of a hooked cf. *Pertica quadrifaria* specimen with locations of Figs. 5B–5G marked. **B**) An acute spine apex without any terminal pore but with degraded cuticle. **C**) An acute apex at which homogenous (arrow) cell walls features are discernible. **D**) Compressed (white arrow) poorly preserved hook in which original plant cuticle (black arrow) is preserved. **E**) Waxy globules (arrows) that are interpreted as melted cuticle. The area to the right lacks this feature. **F**) A poorly preserved non-cuticular area of the hook with a thick (up to 31 μm wide) tube welded to it. Top edge of tube marked by arrow. **G**) Fungal hyphae (arrow) inter-grown with the hook cell walls.

11B, both charred) and those between about 2.75–3.0 mm in length (Fig. 11C–11E, of which Fig. 11C is charred). The smaller sporangial remains fall in the size range for TVFm *Pertica quadrifaria* (2.0–3.0 mm) reported by Andrews and Kasper (1972). The larger sporangia match the length range cited for *Psilophyton forbesii* (4.0–5.0 mm) at the same locality (Kasper et al. 1974). However, the three charred partial sporangial specimens (Fig. 11A–11C) are morphologically similar and each have a strongly incurved apex (Fig. 11G). Despite charring, cellular preservation is poor (Fig. 11H). This is attributable to pre-burning decay, with fungal hyphae found to be rooted into the sporangial walls (Fig. 11I). The uncharred, compressed specimens (Fig. 11D–11F), beyond size and gross morphology, lack any diagnostic characters. The specimen illustrated in Figure 11F shows dehiscence of the sporangium into lanceolate segments (as in Fig. 11A–11C), but the distalmost apices of it (and the specimen shown in Fig. 11E) are absent. Sporangial dimensions of the other TVFm psilophytes include *Psilophyton dapsile* (1.7–2.1 mm in length), *Psilophyton microspinosum* (3.5–4.0 mm in length), and *Psilophyton princeps* (7.5–8.0 mm in length; Kasper et al. 1974).

Charred Lycophyte Material

The only tracheophyte, non-psilophyte TVFm remains is a single leaf assignable to the rhizomatous lycopsid *Leclercqia* (Figs. 12A–12I, 13B). Unlike *Leclercqia* (*complexa*) *andrewsii* from the TVFm (Kasper and Forbes, 1979) and from the late Emsian-age Campbellton Formation, Canada (Gensel and Kasper 2005; Fig. 13E), this single leaf is not laminar. The shaft of the leaf attached to the leaf cushion on the stem extends in a peltate fashion into the flared (hand-like) leaf tip. At the point of attachment, a heel ~ 50 μm long is visible extending below the leaf shaft (Fig. 12A, arrow). The "hand" of the leaf sits at approximately a right angle to the leaf shaft. Five truncated spines extend from the flared leaf-tip, two closely set together and pointing vertically. The remaining three spines are disposed around the leaf tip in a flared hand-like manor. However, damage to the leaf has probably removed a sixth spine that would have angled to the NW of the specimen mirroring the middle spine on the right and side. The spines (Fig. 12B–12D) appear steeply conical and appear to be hollow at the very apex. The longest spine measures 500 μm in length (Fig. 12B)

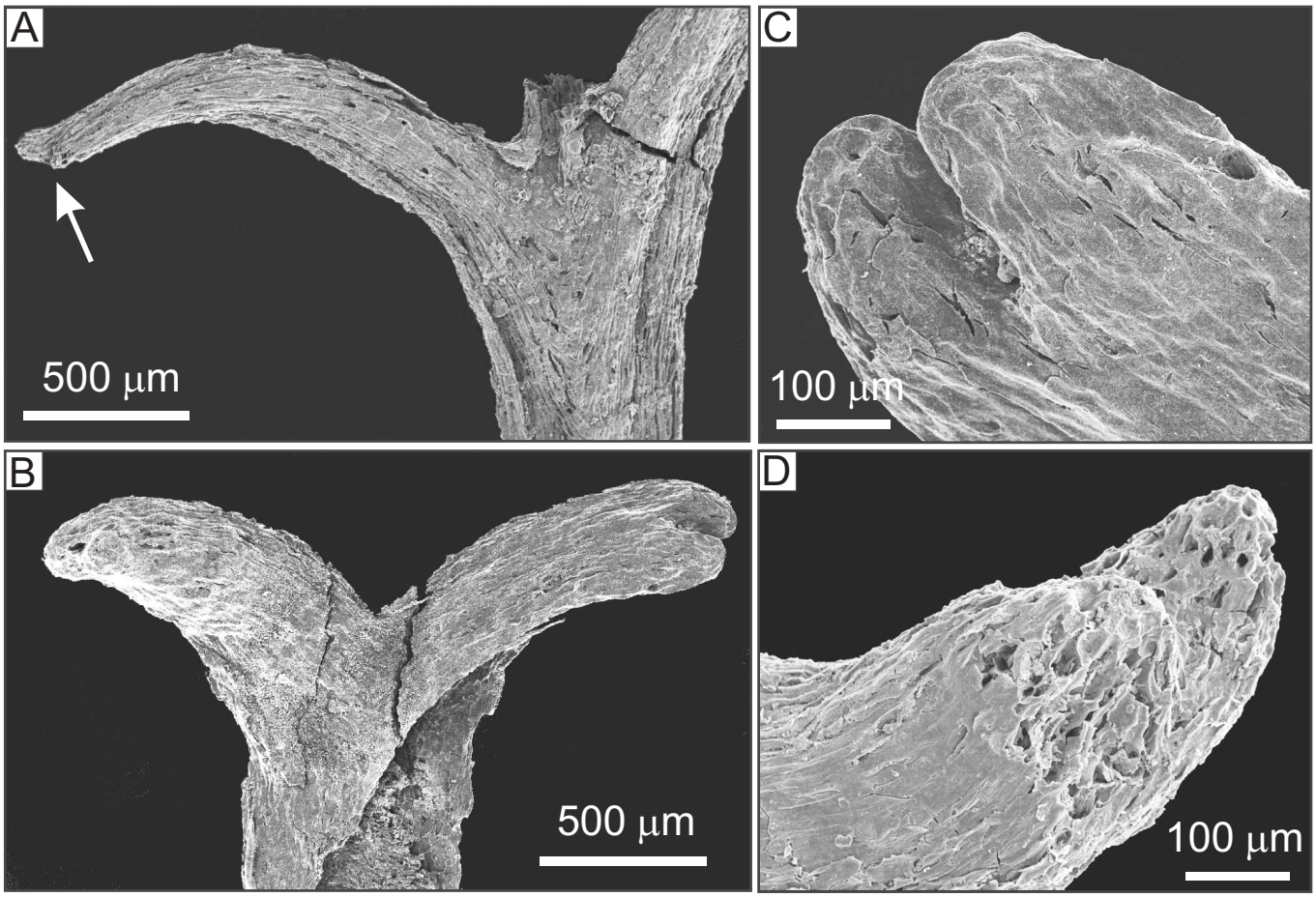

FIG. 7.—Trout Valley SEM images, two charred, 3D preserved, psilophyte appendages with bifid terminations. cf. *Pertica quadrifaria.* **A**) P-S6-S13 (Fig. 5D) arrow indicates bifurcate tip. **B**) P-S6-S, overview of both hooks with bifurcate endings. **C**, **D**) Details of B.

and is probably nearly complete. The remaining spines are all truncated before their terminations. There are two offset scars (Fig. 12E, arrows) on the incomplete leaf shaft. Grierson and Bonamo (1979, fig. 7) illustrate a ligule and sporangial pad for this taxon. The offset nature of the scars in Fig. 12E, out of central alignment on the leaf shaft, are botanically atypical; we do not ascribe them to the remains of organs. While not gelified, the internal anatomy of the leaf is not well-preserved, although cellular structure is discernible in the cuticle (Fig. 12H). The cuticle itself seems to have collapsed and possibly melted into openings such as stomata (Fig. 12F, 12G). The impression that the leaf had been abscised and partially decayed prior to being charred is evidenced by the presence of fungal hyphae (Fig. 12I).

Nematophytes and Coprolites

The largest, most robust mesofossils in the TVFm macerates were either nematophytic or coprolitic in origin. Nematophytic material was entirely prototaxodioid, assignable either to *Prototaxites* or *Nemata*sketum. We are not able to differentiate which taxon due to both preservation and the absence of diagnostic characteristics. Prototaxodioid material stands out as charred due to its blocky and angular (Fig. 14A) and often highly lustrous (Fig. 14B) appearance. Large tubes are often identifiable even under incident light (Fig. 14B). Rounded and eroded fragments (probably through bedload transport) also occur (Fig. 14C), and the characteristic large (~ 30 μm diameter) and small (a few micrometers) tubes (Fig. 14D) may be preserved or not. Specimens of the latter category are either extremely compressed, distorted and fractured, or degraded. Other degraded material includes probable coprolites (Fig. 14E, 14F).

The probable coprolites are typically rounded and have a matte, often fractured surface (Fig. 14E). Most do not preserve readily identifiable features and are interpreted as coprolitic in origin. However, one coprolite (Fig. 14F–14I) contains what appear to be arthropod remains. The filamentous, grooved objects (Fig. 14G, 14H, arrows) may be arthropod setae; this identification is speculative. The other remains (Fig. 14G, 14I) with rows of elongate sockets/raised pustules resemble invertebrate cuticle recovered from the Givetian of New York and that may have come from an archaeognathan insect (personal communication W.A. Shear 2024). Most modern arachnids digest their prey preorally and, as such, cuticle fragments do not enter their digestive systems. However, insects, centipedes, some harvestmen, and some mites may consume solid prey and could be potential progenitors of the coprolite.

Reflectance Data of Maine Devonian Samples

Reflected light microscopy on the TVFm material (Fig. 15) indicates mean random reflectances ranging from R_oV 1.92% to 6.66% (n = 50, mean 4.52%; Table 4). Amongst these samples, bireflectance (i.e., maximum-apparent minimum reflectance) was captured on five specimens for which there was microscopic data. Bireflectance ranged from 0.11 to 2.08% (Table 5). Morphologically, the lowest bireflectance values were expressed by those samples possessing a level of anatomical preservation most typical

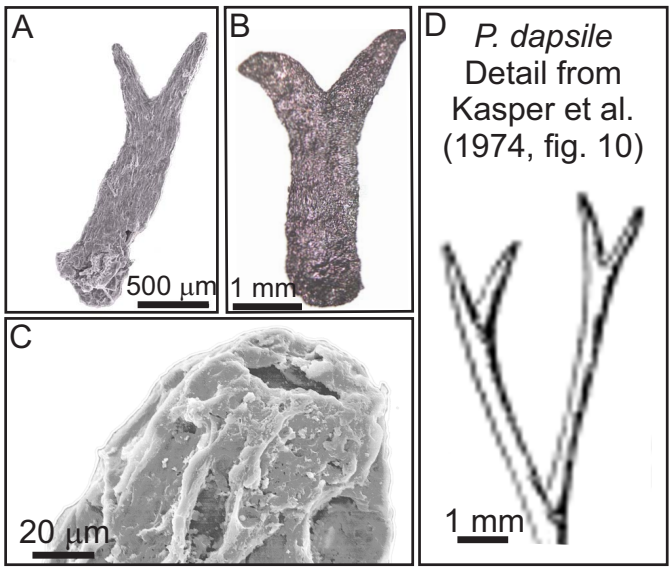

FIG. 8.—Trout Valley SEM (A, C) and incident light (B) images of two charred, 3D preserved, terminal psilophyte appendages. cf. *Psilophyton dapsile.* **A**) P-S4-S16. **B**) P-S6-S12. **C**) Detail of A showing pore at tip of apex. **D**) Detail taken from Kasper et al. (1974, fig. 10) reconstruction of *Psilophyton dapsile*.

of completely charred (vs. partially charred/semifusinitic) fossils (see Scott and Glasspool 2007). Atypically, the highest reflectance values were observed in specimens with vitrinitic or semifusinitic morphologies rather than in those appearing fusinitised.

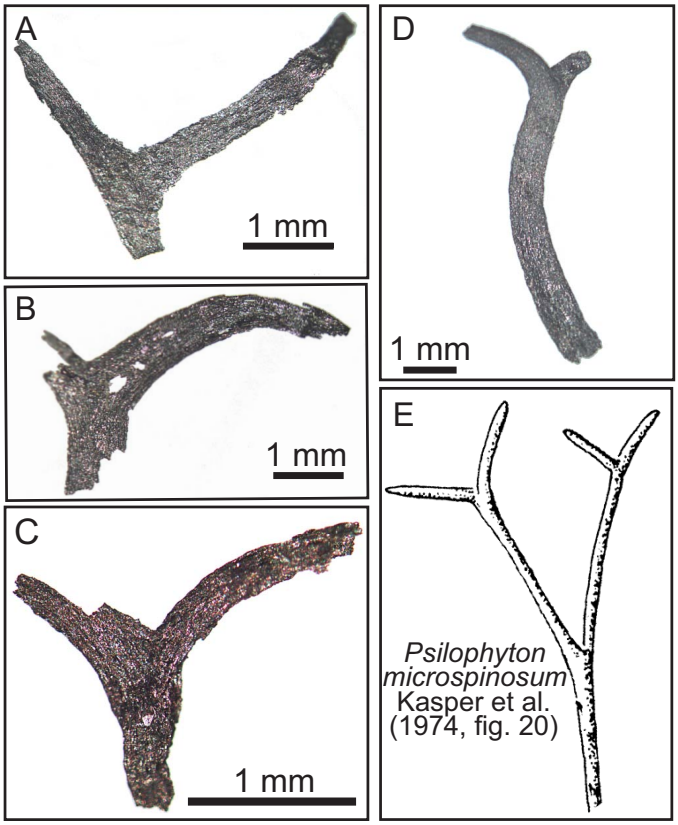

FIG. 9.—Trout Valley incident light images. **A–D**) Four charred, 3D preserved, terminal psilophyte appendages. cf. *Psilophyton microspinosum*. Specimens: A, P-S1-S2; B, P-S1-S1; C, P-S4-S9; D, P-S5-S7). **E**) Detail taken from Kasper et al. (1974, fig. 20) reconstruction of *Psilophyton microspinosum*.

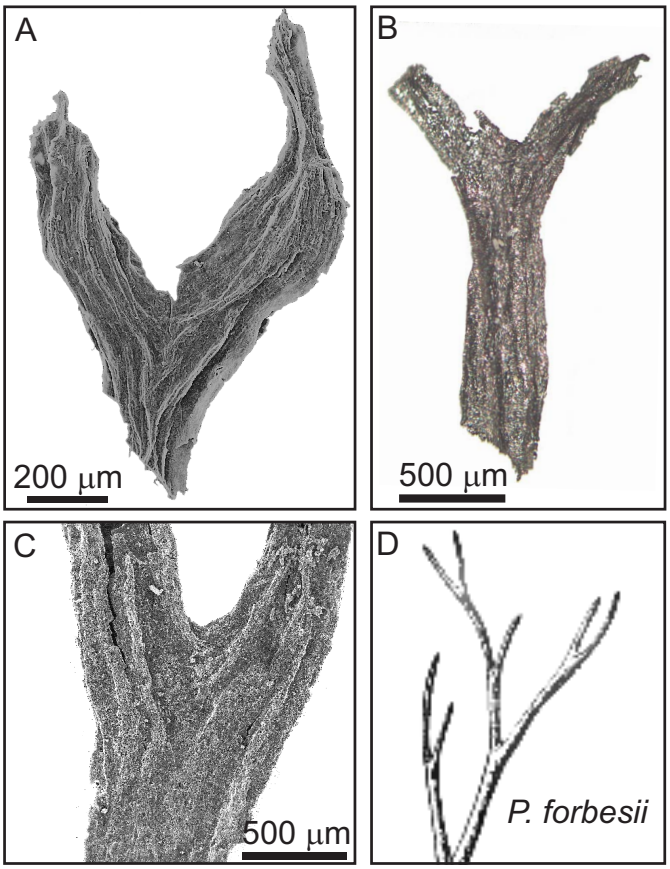

FIG. 10.—Trout Valley images of strongly ribbed terminal appendages with a relatively acute angle of divergence. cf. *Psilophyton forbesii*. **A**, **C**) SEM image of specimens P-S4-S4 and P-S2-S1, respectively. **B**) Incident light image of specimen P-S4-S1. **D**) Detail taken from Andrews et al. (1968, fig. 10) reconstruction of *Psilophyton forbesii*.

Phytoclast Recovery from Other Maine Localities

Samples macerated from the Mapleton Fm., Chapman Fm., Frenchville Fm., Fish River Lake Fm., and St. Froid Lake localities either were barren of phytoclasts, yielded coalified fragments, or were charred. No charcoal was recovered from macerations of either the red or yellow beds of the Mapleton Formation (Fig. 16A–16E), despite the yellow-bed sediments appearing superficially full of heavily oxidized organic detritus. All specimens were vitrinized and, with the exception of one possible lycopsid spine and two coprolites, morphologically unidentifiable. Organic residues from the Chapman, Frenchville, and Fish River Lake (now placed in the Seboomook Fm. upon remapping by Wang 2022) formations yielded no mesofossil remains. The newly mapped St. Froid Lake Formation did yield charred nematophytic and cryptophytic mesofossils from several localities (Fig. 16F–16H; Wang 20274, 20646, 20568, 20600, and 20657); one locality (20205) yielded no charred remains. All phytoclasts are of diminutive size (Table 6) and no unquestionable embryophyte remains were identified.

DISCUSSION

It is not immediately apparent in incident light whether specimens from the TVFm are charred or only coalified (see Figs. 3A–3E, 4A). Here, identification is, in part, complicated as a result of localized contact heating by late Paleozoic intrusives (R_{oV} 1.6–8.2%; Malinconico 1993a and personal communication 2023) in the area. Even inspection with SEM (Figs. 4C,

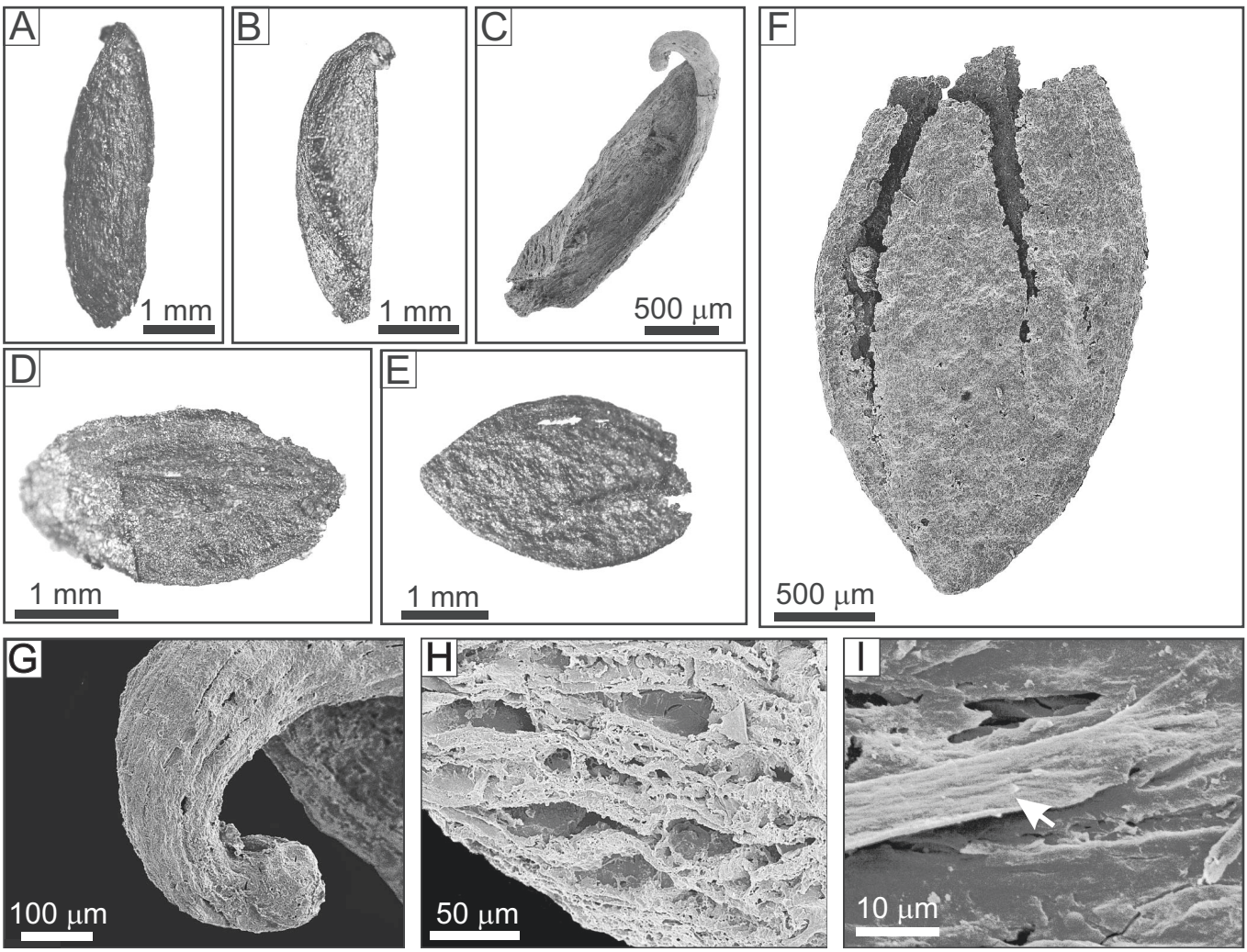

FIG. 11.—Incident light (A, B, D–F) and SEM (C, G–I) images of Trout Valley psilophyte-reproductive structures. **A–C**) 3D, charred anatomically preserved sporangial segments (A, P-S6-S8; B, P-S6-S9; C, P-S6-S10). **D–F**) Compressed sporangia with E and F showing apical dehiscence (D, P-S6-S6; E, P-S6-S7; F, P-S5-S2). **G–I**) Details of Fig. 11C showing apical torsion (G); degradation of sporangial anatomy (H), and fungal hypha welded to sporangium (I).

14C) doesn't necessarily evidence the pre- and post-burial taphonomic processes that operated during the preservation of TVFm material. Imaging using reflected light microscopy, similar to SEM and incident light microscopy, though, offers anatomical and morphological clues into the taphonomic mode of individual specimens. Critically, at higher metamorphic ranks (> low volatile bituminous) where it become difficult to distinguish vitrinite (anisotropic) from fusinite (isotropic) based upon quantitative reflectance data, the state of isotropy provides a tool for such differentiation. This differential character can be assessed through observation of specimen-extinction characters, when rotated in plane polarized light.

The TVFm specimens exhibiting the highest reflectance and fusinitic morphology (e.g., P-S6-S1; Figs. 5C, 6) have a Rmax = 5.07% and exhibit a minimal bireflectance (0.11%). This is well below the predicted bireflectance range expected of vitrinitic fossils of this rank. Organic matter with an Rmax = 5.0% is predicted to exhibit bireflectance ranging from 1.7–4.1% (Fig. 17; Stach et al. 1982, table 4a). Specimens P-S3-S2 and P-S3-S3 have Rmax values of 5.05% and 5.06%, respectively. The values are comparable with specimen P-S6-S1 (Table 5), but these mesofossils are vitrinitic and show no evidence of internal anatomy. These specimens exhibit bireflectances of 1.90% and 2.68%, respectively, and are values that correspond with predictions for vitrinite of this rank (Stach et al. 1982). Specimens with lower Rmax values (e.g., P-S6-S12), but with an inertinitic morphology, exhibit slightly greater bireflectance. Such values are still lower than would be expected of vitrinitic material of this rank. Bireflectance in 2021-S1-S4, with semifusinitic morphology, was less than that of vitrinitic specimens (i.e., P-S3-S2, P-S3-S3), but fell within the low range of expected values for this rank. The relative isotropy/anisotropy of the specimens indicates which were charred prior to burial and fossilization and those specimens which were not burned.

The isotropy/anisotropy of TVFm specimens matches well their morphological characters (Fig. 17). More isotropic specimens invariably appear black and lustrous in incident light (e.g., P-S6-S1, Fig. 5C; P-S6-S12, Fig. 8B). When viewed by SEM (Fig. 6) they exhibit 3D cellular level preservation. Viewed by reflected light microscopy (Fig. 15D, 15E) this anatomical preservation is still apparent, although there is also evidence of brittle cellular fracture (Fig. 15E), which is a characteristic typical of material charred prior to compression. Some specimens display blistering (Fig. 6E) and possible melting of their cuticles (Figs. 8C, 12B, 12F, 12G). These characteristics are indicative of extreme heating (Edwards and Axe 2004). Both SEM and reflected light microscopy, however, demonstrate evidence of decay in all organ types including compression and loss of internal anatomy (Figs. 6D, 12H), fungal/

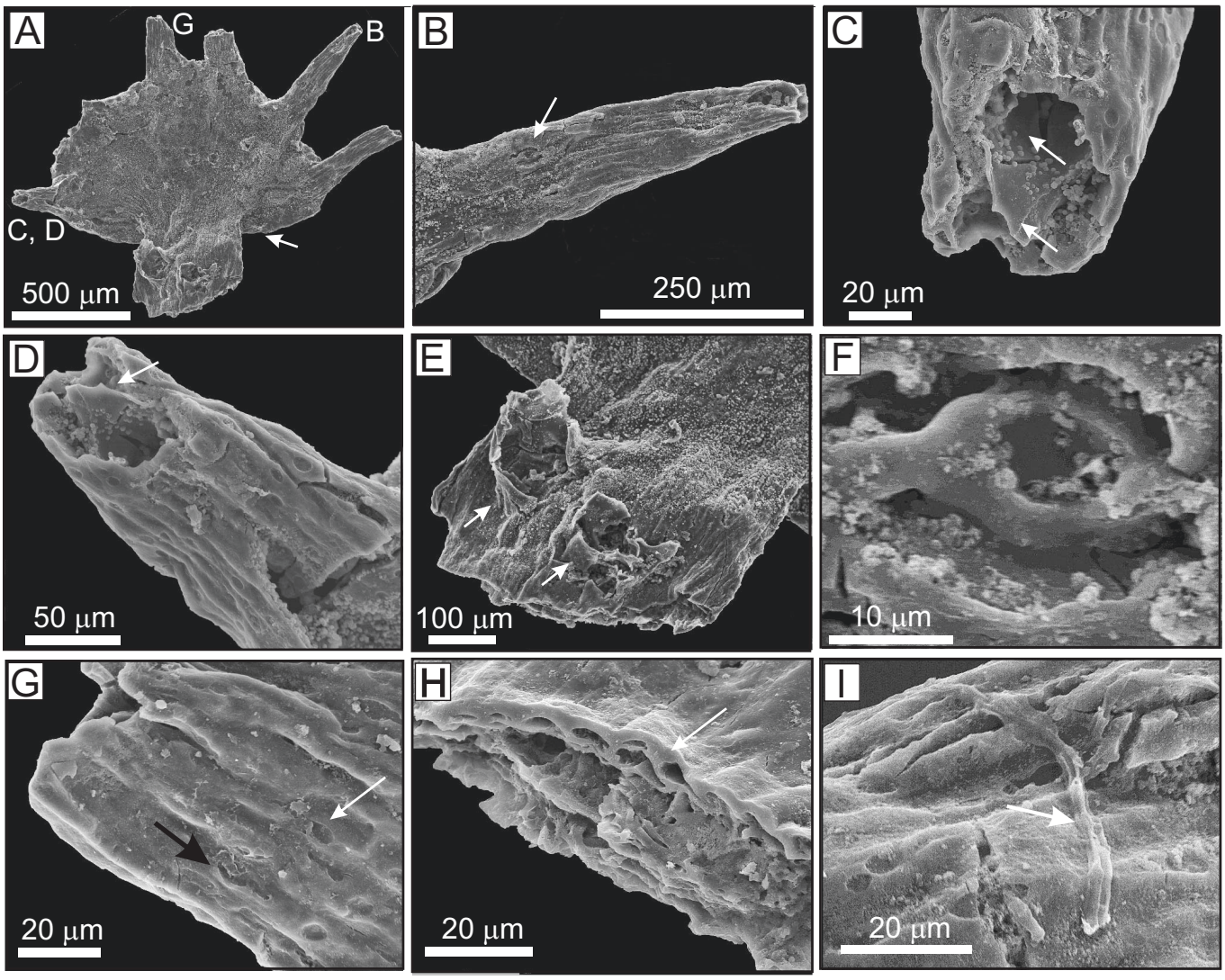

FIG. 12.—Trout Valley SEM images of one charred, 3D preserved, distal portion of a lycopsid leaf *Leclercqia* cf. *andrewsii.* **A**) P-S4-S8, overview. Arrow indicates a heel (~ 50 μm long) of the leaf blade protruding below its peltate, near right-angled attachment to the leaf shaft. **B–D**) Hollow spines extending from the blade of the leaf. Arrow on B indicates stomata (see Fig. 9F). Arrows on C indicate large diameter, smooth-walled interior of spine. Arrow on D indicates brittle fracture. **E**) Arrows indicate two eruptions of tissue from the shaft of the leaf (see text). **F**) Possibly, a poorly preserved stomata. **G**) Arrows indicate possible cuticular melting and blistering. **H**) Compressed tissues of the leaf shaft, arrow indicates cellular impressions preserved by the cuticle. **I**) Fungal hypha welded to the leaf.

nematophytic hyphae (Figs. 6F, 6G, 11I, 12I), shrinkage of cuticle and possible desiccation (Figs. 8C, 11A–11C, 12G), and cellular delamination (Figs. 6G, 11H, 15D, 15E). Evidence of decay is supported by the occurrence of coprolites in these assemblages (Fig. 14E–14I). Sporangia in the sample show signs of having been at a post-reproductive stage. This is evidenced by the fact that sporangial loss is represented by just a scar pad in *Leclercqia* (Fig. 12E), the apparent dehiscence of sporangia (Fig. 11E, 11F), and the separation of sporangia into individual segments (Fig. 11A–11C). Collectively, these features indicate charring resulting from wildfire activity was part of the taphonomic pathway of some specimens, and that this charring predominantly occurred to a post-reproductive, senesced vegetation that had begun to decay. These conditions are found as part of a relatively newly formed litter layer, but the temperature at which this material burned is unknown.

The minimum temperature of TVFm wildfire activity cannot be investigated. This is because the high rank of the sediments overprints data on both partially charred and even fully charred specimens at low temperatures. Similarly, an interpretation of fire temperature of the SFLFm fossils (Aroostook County, northern Maine), based on our reflectance data, is complicated by the high regional rank of these rocks (Fig. 1). Rank maturation of three of these localities (Wang 20568, 20600, 20657) falls between the R_G 3.0 to 4.0% isograds as predicted by Malinconico (1993a, 2023). In contrast, the remainder are in basins in the area associated with Ro_v 1.0–1.2% (Fig. 1).

The taphonomic pathway of the uncharred specimens is not uniform. Across the TVFm, the maximum mean vitrinite reflectance has been observed to vary by 6.6%, from medium volatile bituminous to meta-anthracitic (Malinconico 1993b and personal communication 2023). The mean random reflectance reported in the current study ranges from low volatile bituminous to anthracitic/meta-anthracitic (1.92–6.66%; Table

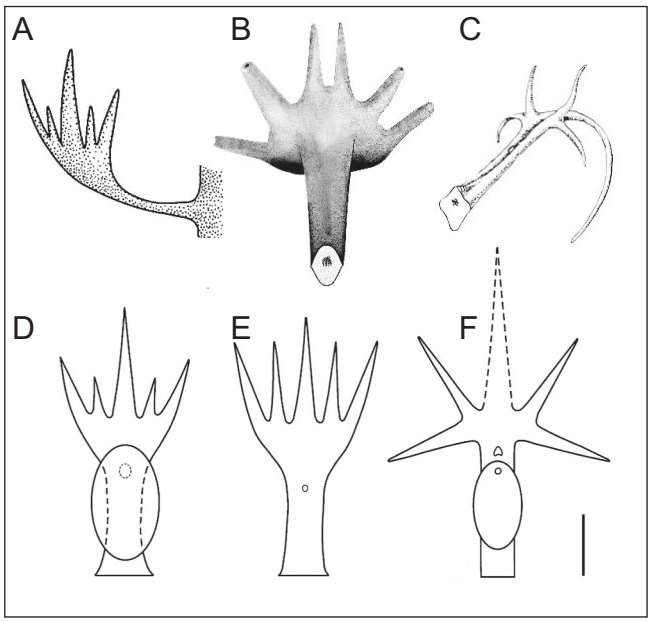

FIG. 13.—Line drawings of *Leclercqia* spp. **A**, **D**) *L. andrewsii* from the Emsian Campbellton Formation of New Brunswick. **B**, **E**) *L.* cf. *andrewsii* and *L. andrewsii* respectively from the Emsian–Eifelian Trout Valley Formation of Maine. **C**, **F**) *L. complexa* from the Givetian Panther Mountain Formation of New York. Figures (A, D–F) are taken from Gensel and Kasper (2005) and C from Bonamo et al. (1988). B is newly reconstructed from the specimen illustrated in Fig. 12.

4). These variations in reflectance far exceed the range that might be expected from burial diagenesis alone. From the range of reflectances and the "*smooth non-granular non-coked texture*" of her samples, Malinconico (1993a) proposed that "*all or part of the Trout Valley Formation had been heated by an unidentified thermal event to temperatures above the coking range of coal before being subjected to later very local contact metamorphism by dikes and sills*". Differential degree, multi-episode heating events seem probable and a satisfactory explanation of the range of reflectances found in these rocks (Table 4). The presence of a discrete, yet vitrinized vascular strand-bearing impressions of original anatomy (Fig. 4), and which is partially ensheathed therein but separate from outer cortical tissues (also vitrinized), is highly unusual. It is possible that the multi-episode heating may have had a role to play in the development of this feature. However, such an interpretation would suggest that at least some of this external heating occurred contemporaneously, or in close contemporaneous proximity, with the senescence of the fossils, so that impressions of cellular level anatomy might be preserved.

Affinities of Charred Vegetation

Twenty-one different plant genera occurring as plant adpression fossils have been documented from the Devonian of Maine (Table 3; plus cf. *Protolepidodendron* sp. from the SFLFm). Of these 21 taxa, six are lycophytes, four cladoxylopsids, two basal Euphyllophyta (*sensu* Kenrick and Crane 1997), two rhyniophytes, one an aneurophyte, one a bryophyte, one a nematophye, and four are of uncertain affinity (*incertae sedis*). Thirteen taxa are not identified beyond the generic level and, of these, three are only tentatively assigned that level of taxonomic confidence. The enigmatic mesofossil *Pachytheca* sp. is the only plant reported from Pragian-age rocks (Pšenička et al. 2021), while the cladoxylopsids are reported solely from the Eifelian Mapleton Fm. (Kasper et al. 1988). The clades most frequently described at the level of species are the Emsian to Eifelian-age basal euphyllophytes and the lycophytes. This phylogenetic distribution is strongly reflected in the charred mesofossil remains from the TVFm.

Most of the identifiable charred remains in the current study are basal euphyllophytes, particularly the most distal portions of the plants (Figs. 3, 5–11). The only other embryophytic charcoal encountered, to date, is a single lycopsid leaf (Fig. 12). However, nematophytes, including prototaxodioids, are frequently charred. They occur not only in the TVFm but also the SFLFm; the other remains from the latter formation are small cryptophytic or bryophytic fossils, some comparable with the lichenoid *Spongiophyton* sp.

The taxonomic distribution in the TVFm is in accord with the prevailing concepts of basal euphyllophytes growing in turfed-in stands, interspersed with prototaxodioids and rarer lycopsids, interacting with an invertebrate community across this estuarine landscape (Selover et al. 2005; Allen and Gastaldo 2006; Gastaldo 2016). Of the five basal euphyllophyte macrofossil taxa (*Pertica quadrifaria*, *Psilophyton dapsile*, *P. forbesii*, *P. microspinosum*, and *P. princeps*) identified in Baxter State Park, only *P. princeps* does not appear in our samples as charcoal. However, the taphonomy of the charred fossils does not suggest that living plants were burned. Rather, senesced and even partially decayed remains (predominantly terminal appendages and reproductive structures) were pyrolized. This may correspond well with the pronounced seasonality forecast for this locality (Allen and Gastaldo 2006). During seasonally drier intervals a litter layer predominantly comprised of basal euphyllophyte and lycophyte organs, but interpenetrated by prototaxodioid nematophytes, was combusted as fuel moisture levels were lowered because of drying. The presence of terrestrial predatory arthropods (perhaps centipedes or insects) in this setting is confirmed through coprolites and indicates a multi-tiered food-web thriving in this coastal environment.

No higher order embryophytes were recovered as charcoal from the SFLFm. These mesofossils were, where identifiable, exclusively nematophytic (prototaxodioid), lichenoid (*Spongiophyton*), or had a cryptophytic/liverwort-like morphology. This taxonomic makeup may reflect taphonomic biases of the depositional environment of this formation, interpreted as a transitional shallow nearshore-marginal marine, or coastal lacustrine setting. Alternatively, the composition may indicate a restricted ecology exploiting a transitory or mobile environment that was combusted prior to colonization of the setting by advanced embryophytes. Here, plant debris was transported as fluvial suspension load, settled to the sediment-water interface in a nearshore or estuarine setting, and subsequently decayed and then were preserved there under low oxygen conditions and periodic input of coarser clastics. Of all the fragments analyzed from Maine, the prototaxodioid charcoal has the smallest surface area to volume (i.e., it is blockier). Charcoal often exhibits an inverse grading in sedimentary deposits. There are several reasons why this might be the case. Larger fragments are deposited after smaller clasts settle, taking longer to waterlog and remaining buoyant longer (Nichols and Jones 1992). Secondly, the temperature at which these plants were burned, and the salinity of the depositional environment, also play a significant role in the rate of charcoal sedimentation. There is an initial density decrease as a function of water loss below charring temperatures of 300°C which, thereafter, is followed by an increase in clast density (300–350°C) as a consequence of shrinkage (Vaughan and Nichols 1995). Depending on the setting in which waterlogging and sedimentation occurs, more charcoal per unit time settles under freshwater conditions than under salinities. Hence, fractionation of clasts in response to one or more of these factors may account for the preponderance of nematophytes in this unit. We note that these observations are rarely considered when evaluating transported mesofossil assemblages, influencing the available phytoclast composition that bears on their interpretation and extrapolation.

One of the enigmas of Middle Devonian fire, not just in Maine but more globally, remains the lack of evidence of charred cladoxylopsids (Lu et al. 2021). Cladoxylopsids were short-lived and non-woody, possessing a largely parenchymatous and easily decayed trunk, but some (e.g., *Calamophyton*) grew to at least 2–4 m in height (Giesen and Berry 2013). During their growth each

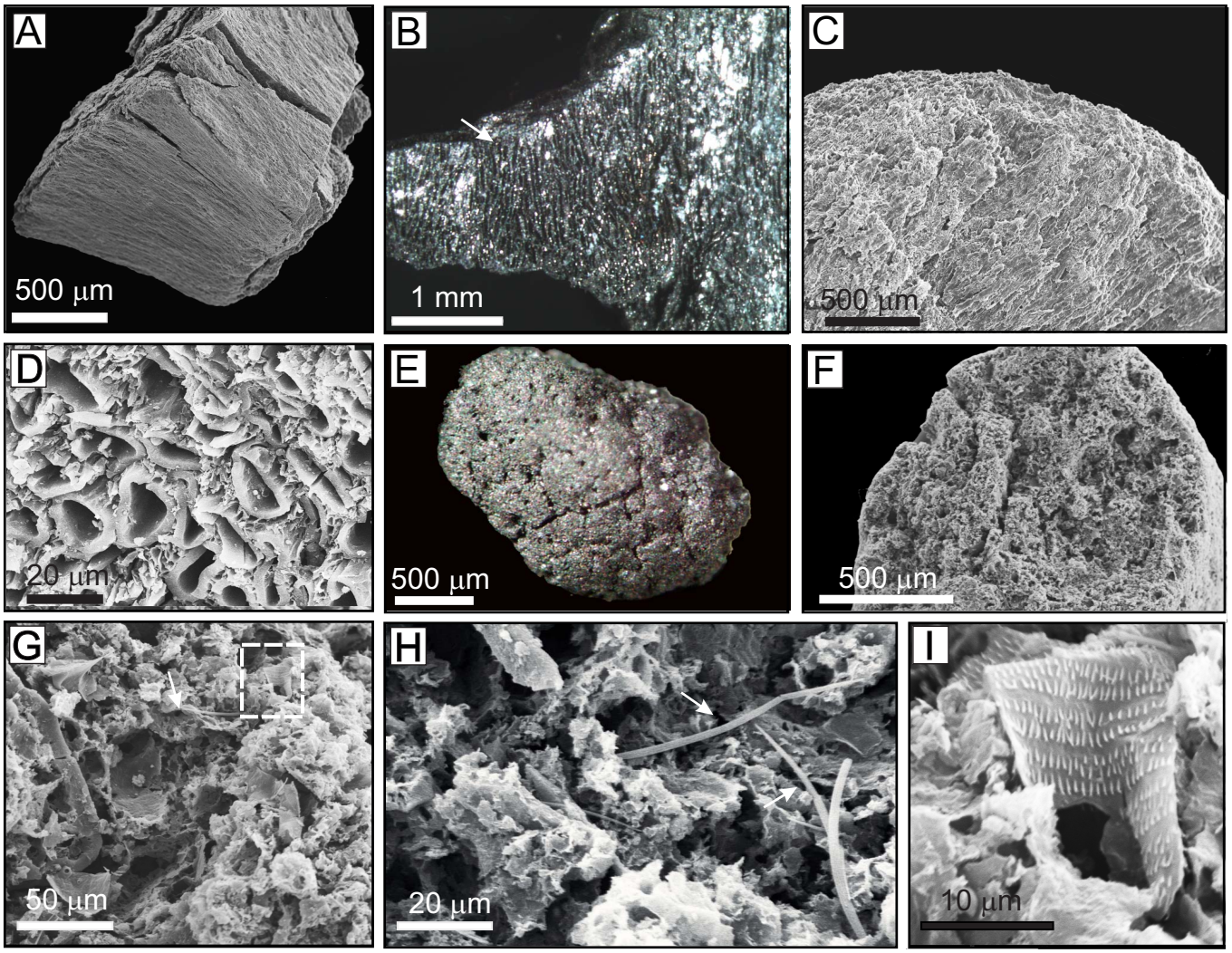

FIG. 14.—Nematophytic and coprolitic remains from the Trout Valley Formation. **A–D**) Charred, cubic-blocky, anatomically preserved prototaxodioid fragments (*Prototaxites* spp. or *Nematasketum* spp.). A) SEM of large cubic prototaxodioid fragment reminiscent of modern charcoal (2021-S4-S7). B) Incident light image of prototaxodioid fragment demonstrating high, silky luster (arrow indicates large prototaxodioid tubes; 2021-S2-S1). C) An SEM of an eroded and rounded prototaxodioid fragment (2021-S4-S13). D). An SEM of anatomically preserved, large and small nematophytic tubes (2021-S1-S4). **E**) Incident light image of a coprolite showing matte texture (2021-S4-S10). **F–I**) SEM images of a coprolite with arthropod remains. F) An overview image (2021-S4-S1). G) A higher magnification image of F) with arthropod remains: arrow indicates a seta, boxed area indicates location of Fig. 10I. H) Several setae preserved in the coprolite (arrows). I) Expansion of boxed area in Fig. 10H showing an ornamented fragment of arthropod cuticle.

Calamophyton tree would have shed between 700–800 branches measuring about 50 cm in length, producing an abundance of abscised material (Davies et al. 2024). This abscised debris accumulated passively in ever wet and waterlogged soils without the influence of strong flowing currents (Stein et al. 2012, 2020; Davies et al. 2024). However, there is also evidence for cladoxylopsid growth in better oxygenated environments alongside archaeopteridaleans (e.g., Cairo, New York; Stein et al. 2020). In Svalbard, lycopsids dominated the wet soils of the Middle Devonian. Cladoxylopsids, while expected, have not been found (Berry and Marshall 2015). These divergent ecological niches and the propensity for these plants to generate large volumes of shed debris should have ensured a new potential source of fuel for wildfires in the Middle Devonian. Evidence for this, including from Maine, is lacking. The cladoxylopsids haven't been reported as macrofossils from the TVFm but were dominant in the Eifelian age Mapleton Fm. flora (Schopf 1964). The fine-to-medium grained, yellow-gray silty sandstones of this formation contain abundant comminuted millimeter-to-centimeter sized plant material. From vitrinite reflectance data (Fig. 1) these sediments are of medium volatile bituminous rank (Malinconico 1993a), a condition confirmed on maceration by the appearance of *Grandispora* sp. megaspores. Given the flora, rank, and sedimentology of these deposits, the presence of mesofossil charcoal might have been expected. This is not the case, and the Mapleton Fm. remains another cladoxylopsidalean environment not yielding microscopic evidence of wildfire, to date.

Similar to the enigmatic absence of cladoxylopsid charcoal, many Middle Devonian coals have low, or no, inertinite content (Diessel 2010; Glasspool and Scott 2010; Glasspool et al. 2015; Lu et al. 2021). Coals from this interval are frequently dominated by liptinitic macerals, particularly cutinite. They have been described in the literature as liptobioliths (Song et al. 2022), a term used much earlier by Potonié (1910) to characterize accumulations of plant resin or waxes. That author discusses the extant genus *Sarcocaulon*, a southern African succulent that can have a waxy coat greater than 1 cm thick (Barthlott et al. 2017). Here, following decay, it may comprise a shell of just these waxy deposits that can then be concentrated by wind or water

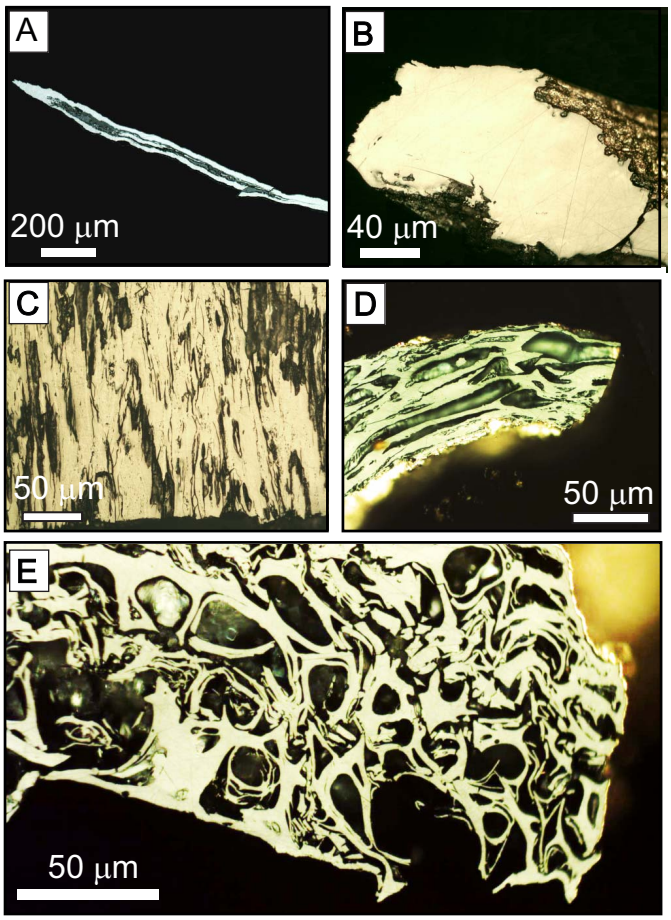

FIG. 15.—Uncalibrated and luminosity modified, oil immersion, reflected light images of Trout Valley mesofossils. **A**, **B**) Uncharred specimens showing vitreous, gelified anatomy (A, P-S3-S3; B, P-S1-S2). **C**) Poorly preserved prototaxodioid tubes showing evidence of compression and alteration (2021-S1-S4). **D**) The apical internal anatomy of a hooked appendage assigned to cf. *Pertica quadrifaria* (P-S6-S1). **E**) The internal anatomy of a hooked-appendage shaft showing cell-wall lamination and separation, and with many cells show brittle fracture bogen structures (P-S6-S12).

into a deposit such as the "denhardtite"/near pyropissite of Kenya (Potonié 1910; Gerschel et al. 2018). The origin of liptobioliths/paper coals and waxy pyropissite deposits remains debated (e.g., Gerschel et al. 2018; Mousa et al. 2022). But taphonomic filtering is frequently invoked and may be the direct effector of the low Middle Devonian inertinite contents.

Significance of Charcoalified Maine Plant Fossils

The Emsian–Eifelian age TVFm charred fossils fall within the 'charcoal gap' of Scott and Glasspool (2006), which they defined by a paucity of charcoal through the Middle Devonian. The absence of a suitable potential fuel source had been excluded by these authors as a contributor to this 'gap' because the first appearance of wood (secondary xylem) is reported at ~ 407 Ma during the Emsian (Gensel 2018; Pfeiler et al. 2021; Strullu-Derrien et al. 2023). The appearance of wood, albeit in small relative quantities relative to the plant bodies in which it formed, is penecontemporaneous with deposition of the TVFm sediments. However, the earliest record of an arboreous growth habit comes slightly later from the Middle Devonian (Stein et al. 2012; Davies et al. 2024). By the earliest Frasnian (~ 382.7 Ma), vegetation more broadly had spread into less moisture-constrained environments, most notably following the appearance of the massive woody archaeopteridaleans (Gensel et al. 2020).

TABLE 4.—*Reflectance (RoV = Mean random reflectance in oil) data from the Trout Valley Formation. Samples labeled TC from "The Crossing", those labeled WB from "Wadleigh Brook", S#S# are mesofossils analyzed microscopically.*

Sample #	RoV Mean (%)	Sample #	RoV Mean (%)
P-S4-S1	1.92	WB-SV1	4.81
TC-16	2.95	TC-1	4.82
WB-S4	3.00	WB-S5	4.85
WB-SV3	3.23	TC-6	4.93
TC-14	3.23	WB-SV2	4.94
P-S5-S1	3.29	TC-8	4.96
P-S4-S2	3.32	P-S3-S1	5.00
P-S6-S12	3.32	WB-S11	5.02
2021-S1-S4	3.33	TC-12	5.02
WB-S2	3.40	P-S1-S1	5.04
P-S3-S2	3.42	TC-3	5.14
WB-S5	3.71	TC-11	5.21
TC-15	3.74	TC-10	5.23
P-S3-S3	3.82	WB-S3	5.25
WB-S3	3.87	WB-S12	5.31
WB-S2	4.00	TC-2	5.33
WB-S6	4.10	WB-S1	5.36
WB-S1a	4.17	WB-S6	5.42
P-S6-S3	4.18	TC-4	5.64
P-S6-S1	4.35	WB-S10	5.68
P-S6-S8	4.36	WB-S9	5.69
TC-17	4.40	TC-5	5.83
TC-9	4.44	WB-S7	6.06
TC-7	4.47	WB-S8	6.18
TC-13	4.68	P-S1-S2	6.66

These evolutionary milestones resulted in increased levels of fuel and one would expect to find greater evidence of wildfire, such as charcoal/inertinite. However, the Middle Devonian, although a somewhat cooler episode of the broader Devonian greenhouse interval (Scotese et al. 2021), does not, as yet,

TABLE 5.—*Bireflectance (Maximum minus apparent minimum reflectance in oil) data from five specimens within the TVFm mesofossils analyzed microscopically. The presence of multiple bireflectance values for P-S6-S12 is a consequence of sampling different localities in the specimen showing a cline of morphology from semifusinite to fusinite.*

Sample #	Rmax%–Rmin% (Bireflectance)	Description
P-S3-S2	5.05–3.15 (1.90)	cf. *P. quadrifaria* hook—vitrinitic, but with some surface anatomy (Fig. 3B)
P-S3-S3	5.06–2.37 (2.68)	Psilophyte axis, that appears superficially charred and 3D.
2021-S1-S4	3.60–2.88 (0.72)	Prototoxaodioid–semifusinitic, compressed and imperfectly preserved (Fig. 13C)
P-S6-S8	4.25–4.09 (0.16)	Psilophyte anatomically preserved sporangial fragment (Fig. 11C)
P-S6-S1	5.07–4.96 (0.11)	Anatomically preserved cf. *P. quadrifaria* hook but with areas of compression and decay (Fig. 6)
	3.88–3.34 (0.54)	
	3.73–3.26 (0.47)	
P-S6-S12	3.50–3.13 (0.37)	Anatomically preserved cf. *P. dapsile* hook (Fig. 8B).
	3.31–3.03 (0.29	
	3.52–3.28 (0.24)	

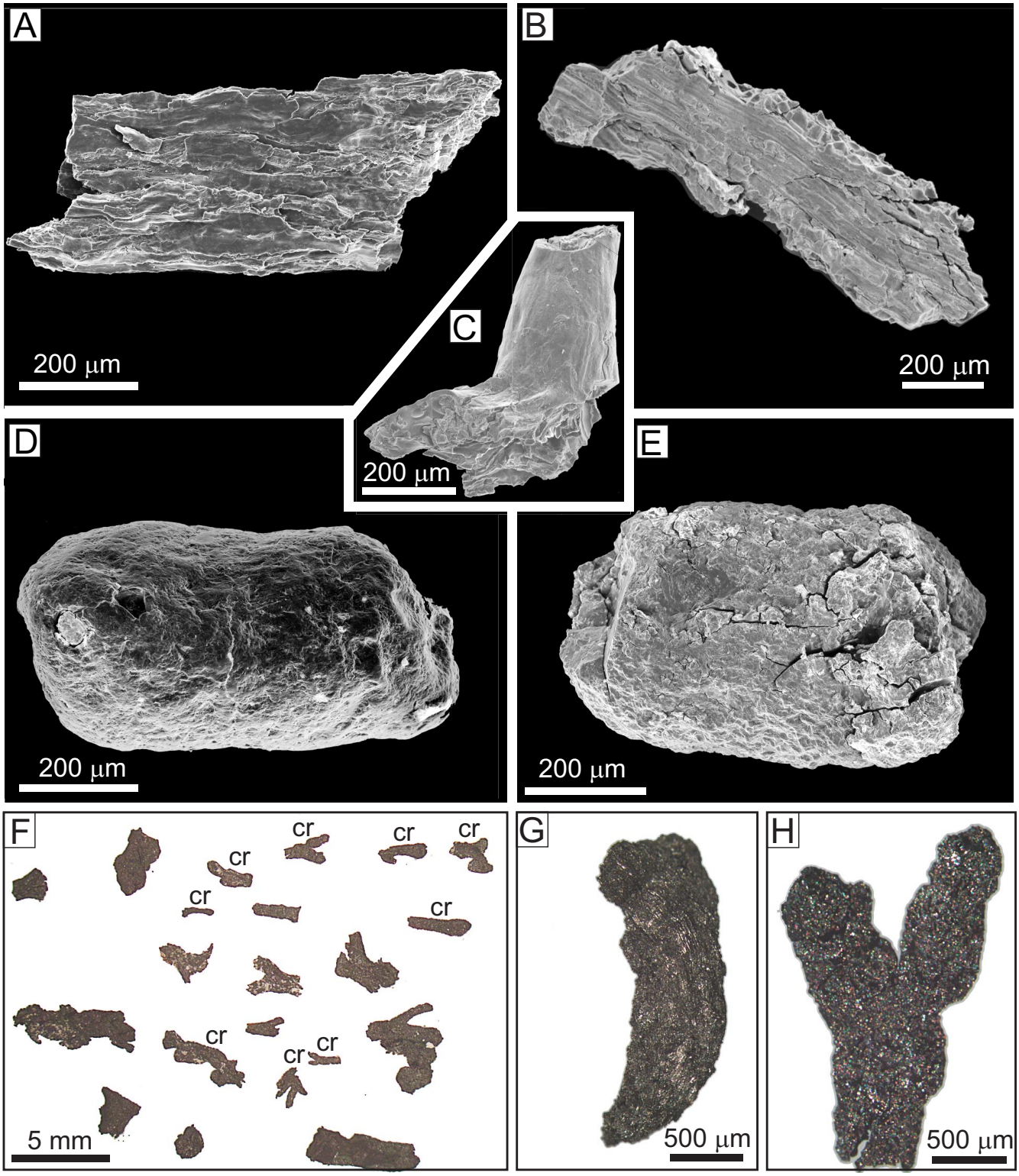

FIG. 16.—Mesofossil remains from Mapleton and St. Froid Lake Formation. **A-E**) Yellow Beds, Mapleton Fm. Winslow Farm. SEM images. **F-H**) SFLFm Incident light images. **A-B**) Vitrinized fragments bearing slight impressions of original cellular anatomy. **C**) Vitrinized spine, possibly lycopsid in nature. **D, E**) Coprolites. **F, H**) Charred cryptophytic (cr) and unclassifiable mesofossil remains from Wang locality 20274, **H**) is detail of central top specimen in **F**) and is morphologically similar to *Spongiophyton* sp. **G**) charred prototaxodioid fragment from Wang locality 20657.

TABLE 6.—*Mesofossil recovery from the St. Froid Lake Formation.*

Wang locality #	Mesofossil description
20274	Nine charred cryptophytes (Fig. 15F, cr) including a specimen comparable with *Spongiophyton* (Fig. 15H) and other unclassifiable fossils. The largest specimen measures ~ 6.5 mm in length.
20646	Thirteen charred unclassifiable mesofossils all sub-millimeter sized in scale
20568	Twenty-nine mesofossil fragments, of which one (~ 2 mm in length) is a charred prototaxodioid, while the nature of the others (rounded specimens < 1 mm diameter and three elongate specimens < 1.5 mm in length) is equivocal.
20600	Twelve mesofossil fragments of maximum 2 mm in length, all except one a charred prototaxodioid is taxonomically unclassifiable.
20657	Seven charred mesofossil fragments, the largest a remnant of a charred prototaxodioid measures 3 mm in length

support an extensive record of charcoal/inertinite (Diessel 2010; Lu et al. 2021) and, hence, fire. The exceptions to this record are those of northern Maine from the TVFm and the SFLFm, adding extra significance to the current report.

Charred TVFm specimens also have revealed features unreported in the compression fossil assemblage. These features include the uniquely bifurcate tips of some *Pertica*-like appendages (Fig. 7), the function of which remains unclear. Similarly, the pore discernible in the charcoalified remains of *P. dapsile* (Fig. 8C) is unreported until now. The presence of a curled, beak-like apex at the distal end of psilophyte sporangial (Fig. 11A–11C, 11G) segments also remains, as far as we are aware, undescribed. What is of interest are the well-preserved stomata in *Leclercqia* that allow for a more refined anatomical comparison with other contemporaneous localities (e.g., Gensel and Albright 2006), and the unique leaf morphology.

The structure of TVFm *Leclercqia* leaves (Figs. 12, 13C) is divergent from other records of this genus from the formation (Kasper et al. 1974) and from strata of comparable age and sedimentology (Meyer-Berthaud et al. 2003). Most overtly, the single specimen figured herein appears to have had six spines, although variation in process number has been reported in other *Leclercqia* of this age (Banks et al. 1972; Gensel and Albright 2006; Xu et al. 2020). The charred Baxter specimen shows the leaf lamina (Fig. 12A) attached to the shaft in a peltate manner so that there is a heel (Fig. 12A) extending below it indicating that the leaf is not a planar structure. The spines of this specimen also appear to be 3D and rigid, appearing hollow for at least 2/3rds of their length (Fig. 12B–12D). Lastly, this specimen possesses two scars on the shaft of the leaf (Fig. 12E). Their offset alignment is unusual and, hence, it is unclear how they compare with other specimens of this genus where two pads (sporangial and ligule) are discernible, aligned one behind the other.

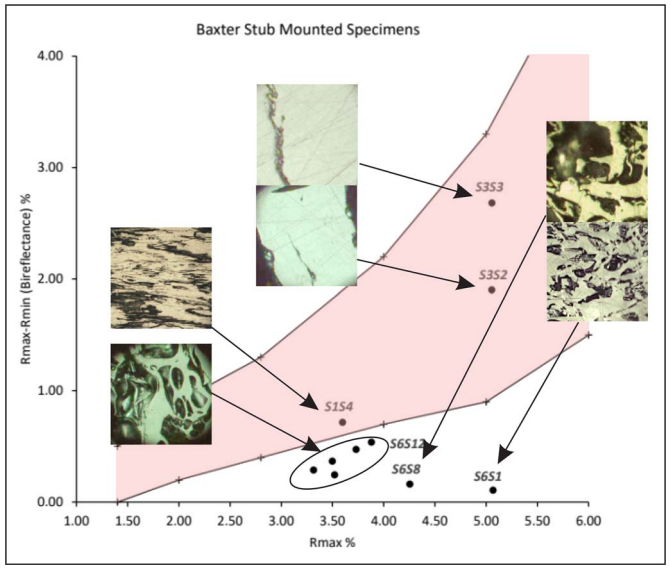

FIG. 17.—A comparison of fossil anatomy and maximum reflectance (Rmax%) plotted again bireflectance (Rmax%-Rmin%). Pink area = predicted range of bireflectance in relation to maximum reflectance (Data from Teichmüller et al. 1979; Stach et al. 1982, table 4a). Specimen color does is not proportional to reflectance.

RECONSTRUCTED TROUT VALLEY FORMATION LANDSCAPE

A reconstruction of the Trout Valley landscape is presented as it may have appeared in the Emsian–Eifelian during the deposition of these estuarine sediments and the fossils they bear, based on previous documentation over the decades and results of the current study (Fig. 18). While it remains proximal to the estuarine setting, the volcanic source of the Traveler Rhyolite underwent erosion since its active formation in the early Emsian (407 ± 3 Ma; Bradley et al. 2000) and was a prime sediment source comprising the TVFm after the ensuing ~ 14 Ma (Allen and Gastaldo 2004). However, it remained a dominant feature of this near-shore coastal setting, an understanding of this relationship based on the onlapping of the TVFm rocks (Allen and Gastaldo 2004). We envisage the vegetation to have been dominated numerically by monotypic, turfed-in stands of psilophytes, including *P. quadrifaria*, associated with other floral elements thriving in close proximity. Noticeably in the foreground, at a slightly higher elevation, are the rhizomes of *Leclercqia*, growing through the recently senesced litter and nematophytic ground cover. As discussed, *Leclercqia andrewsii* from the Emsian Campbellton Fm. of New Brunswick has been reconstructed with laminar leaves (Gensel and Kasper 2005; Fig. 13A, 13D), while *Leclercqia complexa* has a more 3D appearance (Bonamo et al. 1988; Fig. 13C, 13F) much like the recently reconstructed *Leclercqia scolopendra* (Benca et al. 2014). *Leclercqia* from the TVFm (Kasper and Forbes 1979) has been assigned to *L. andrewsii* (Gensel and Kasper 2005; Fig. 13E). The single charred lycopsid leaf is assignable to *Leclercqia* (Fig. 12). However, it is atypical of *L. andrewsii* having at least six spinose appendages and the leaf shaft attached to the hand in a semi-peltate manner (Fig. 13B). Additionally, the hollow-tipped, spines (Figs. 12B–12D) appear stiff, more 3D and more rigid than those illustrated for *L. andrewsii*. However, we have chosen to reconstruct the estuarine marsh with a *Leclercqia* based on more complete regionally contemporaneous assemblages (Gensel and Kasper 2005; Gensel and Albright 2006), as compared with our single charred leaf.

In the distance are larger examples of prototaxodioids, probably one of the foci and main sources fuel of any fire and potentially one of the lightning rods that led to its original ignition (Glasspool and Gastaldo 2022b). While visually most eye-catching, we observe that not all nematophytic prototaxodioid fossils were of such large size, but that many documented elsewhere are highly diminutive, even millimetric in size (e.g., Gensel et al. 2020). We envisage the nematophytes, and among them the prototaxodioid nematophytes, as having been a pervasive element of the contemporaneous (and pre-Mid-Devonian) flora that grew intimately related with embryophytes and appear to have been saprophytic upon them (e.g., Fig. 6F, large tube). We envisage each Middle Devonian fire in this estuarine setting to have occurred at the end of a dry period, with the onset of storms breaking a short-term drought igniting accumulated litter across the

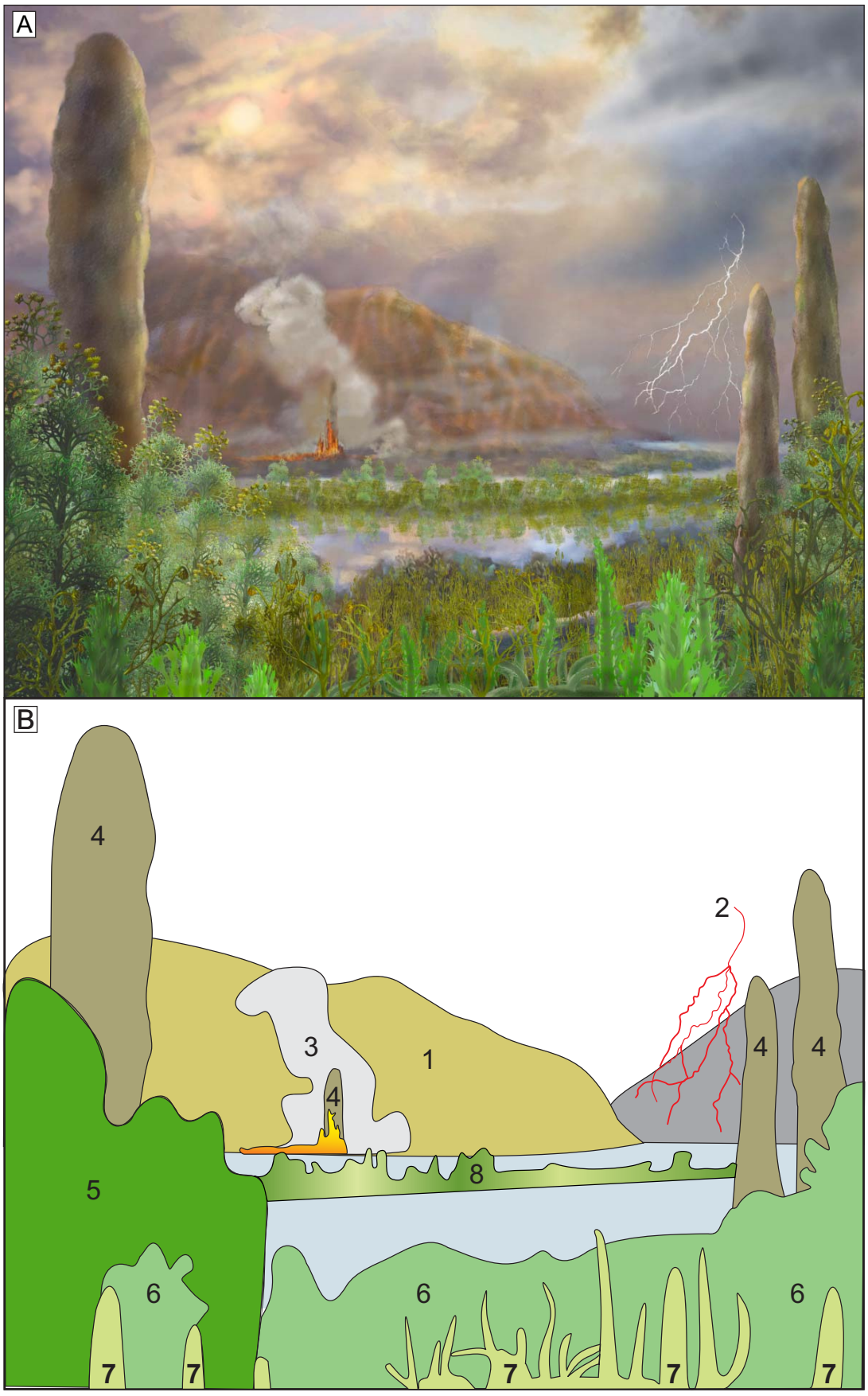

←

FIG. 18.—Reconstruction and explanation of Emsian–Eifelian Trout Valley Formation wetland. **A**) Reconstruction of estuarine marshes during a mid-tidal cycle (Marlene Hill Donnelly, Illustrator). **B**) The eroding Traveler Rhyolite (#1) is the major sediment source for the TVFm (Allen and Gastaldo 2004) where the terrain color mimics that of modern rhyolitic terrain weathering, although in the Middle Devonian coloration may have been different dependent on atmospheric oxygen concentrations and prevailing climate patterns. A lightning storm (#2) has passed over the coastal wetlands. In the distance a ground fire (#3 dark gray), ignited by lightning, burns a prototaxodioid (#4) and senesced embryophyte litter, emitting a smoke plume (#3 light gray) and leaving in its wake a charred and charcoal-rich immature soil. The foreground is dominated by psilophytes including *Pertica quadrifaria* (#5) and *Psilophyton dapsile* (#6) growing amidst prototaxodioids, both living and decaying, and interspersed with the rhizomatous lycophyte *Leclercqia* (#7). A mud bar (#8) in the middle of the tidal channel is populated by dense stands of *Pertica* and *Psilophyton*. However, for illustrative purposes, plant density is lower than would be expected based on modern rhizomatous marsh plants. B) Line art key (18A).

marshes. The ignition of soil litter likely occurred during a neap-tide phase when the emergent land surface was fully exposed over a duration of days.

The reconstructed scenario depicts the sporophyte-growth phase of these plants that follow from an earlier haploid-growth cycle, spore production and the development of diploid plants. The sporophytes had lost their functional parts via abscission and/or their death which were captured in the fire record at an early stage of decay. Amongst this decaying litter were predatory arthropods and early archaeognatha-like insects grazing on available lichens, bryophytes, algae and decayed organics, much like their modern relatives (Sturm 2009). These organisms formed part of an early terrestrial food-web in a dynamic, rapidly changing coastal estuarine landscape of which we now have evidence, due to the improved taphonomic potential for high-fidelity preservation that resulted from being charred.

Although the results used to reconstruct this landscape are based on a limited charcoal data set, they are informed by a compilation of macrofossil (Dorf and Rankin 1962; Andrews et al. 1968, 1977; Andrews and Kasper 1970; Kasper and Andrews 1972; Kasper et al. 1974, 1988; Kasper and Forbes 1979), microfossil (McGregor 1992) and mesofossil (this paper) paleobotanical data, reconstructed in sedimentological context (Gastaldo 1994, 2016; Selover et al. 2005; Allen and Gastaldo 2006). The reconstruction provides a visual representation of Middle Devonian Earth System dynamics in the TVFm marshes, implying feedback between vegetation, wildfire activity, carbon burial, sedimentology, and climate/atmospherics.

CONCLUSIONS

The identification of charcoal can be complicated by the high rank of their associated sediments. An assessment of specimen isotropy provides a robust method of confirming morphological observations made by SEM and incident light microscopy. Reflectance data indicate that the TVFm sediments appear to have undergone several phases of thermal alteration and that rank maturation across the formation is not uniform. These rocks were impacted by small-scale contact-heating events as well as more regional episodes. There is no evidence of the combustion of living plants. Rather, morphological features indicate that a post-reproductive, senesced embryophytic litter, showing signs of the onset of decay, was the main source of fuel. This litter shows evidence of saprophytism and that enigmatic elements of the flora, such as the prototaxodioids, were an important fuel and possible site of fire ignition and nucleation. Coprolites provide evidence of arthropod predation, including the consumption of possible archaeognathan insects, and the basis for an early terrestrial food web.

The charred embryophytic flora of the TVFm matches the compression flora closely in composition and is dominated by *Pertica quadrifaria* and *Psilophyon* spp. There is evidence of charred lycopsids assignable to *Leclercqia*, but this material appears more rigid and three-dimensional than prior reconstructions had suggested for *L. andrewsii*. Such a characteristic may be a function of charring. While there is macrofossil evidence of higher order floral elements (e.g., psilophytes and lycopsids) in the contemporaneous SFLFm these taxa were not found in the mesofossils recovered by maceration. Rather, this assemblage is dominated by small cryptophytic, bryophyte- and lichen-like (e.g., *Spongiophyton*) elements, with much smaller fragments of prototaxodioids that may be indicative of taphonomic filtering. Other Early–Middle Devonian terrestrial sediments have not yielded evidence of wildfire. This includes, perhaps most surprisingly, the Mapleton Fm. Fossil debris, mainly derived from cladoxylopsids, in not overly oxidized sediments that yield megaspores, is abundant at Winslow Farm Quarry in the Mapleton Fm. but yields no charcoal. As yet good evidence of charred cladoxylopsids remains to be found. We reiterate that our assessment of these other northern Maine floras, though, is based on the maceration of small (30 gm) hand samples from which there is a low probability of encountering charcoalified remains.

Our reconstruction of the Trout Valley estuarine landscape during the Middle Devonian is intended not just to demonstrate the floral composition and morphology, but to establish the concept of an integrated Earth System. In this setting we seek to imply the effects of fire on the carbon cycle through its impacts on sedimentation, carbon burial, nutrient mobilization, atmospheric composition, and climate. Fire has been an integral part of Earth System processes since at least the Silurian, and fire has remained an important part of these processes, even during the Middle Devonian, through to the present day.

ACKNOWLEDGMENTS

The authors thank W. Cressler and an unknown reviewer for their comments. We are indebted to Chunzeng Wang, University of Maine Presque Isle, for paleobotanical sampling over the course of his continued geological mapping of Aroostook County, Maine, and providing the authors with material to be processed. Dr. Robert E. Nelson and undergraduate Geology majors including Melissa Trout '01, Caroline Lindley '02, Michael Terkla '02, Jonathan Allen '03, Robert Selover '04, and Kara Robak '20, Colby College, for field and laboratory assistance. The efforts of Chuck Jones, Colby College, with microscope mechanics and maintenance is appreciated. The authors gratefully acknowledge the cooperation of Mr. Irvin 'Buzz' Caverly and Mr. Jensen Bissell, retired Park Directors, and Mrs. Jean Hoekwater, Park Naturalist, for granting permission to salvage Maine's paleontological heritage. For permission to collect we thank Victor Winslow and the Labbe family. The authors are indebted to Drs. Patricia Gensel, Mary-Ann Malinconico and Charles Wellman for their input on the flora and regional setting. Research was supported by Department of Geology endowment funds. NSF EAR 0087433 to RAG, and NSF EAR 1828359 to IJG and RAG.

REFERENCES

ALGEO, T.J., SCHECKLER, S.E., AND MAYNARD, J.B., 2001, Effects of the Middle to Late Devonian spread of vascular land plants on weathering regimes, marine biotas, and global climate, *in* Plants Invade the Land: Evolutionary and Environmental Perspectives: Columbia University Press, New York, p. 213–236.

ALLEN, J.P. AND GASTALDO, R.A., 2006, Sedimentology and taphonomy of the Early to Middle Devonian plant-bearing beds of the Trout Valley Formation, Maine, *in* W.A. DiMichele and S. Greb (eds.), Wetlands Through Time: Geological Society of America, Special Publication 399, p. 57–78.

ANDREWS, H.N. AND KASPER, A.E., 1970, Plant fossils of the Trout Valley Formation: Maine Geological Survey Bulletin, v. 23, p. 3–16.

ANDREWS, H.N., KASPER, A.E., FORBES, W.H., GENSEL, P.G., AND CHALONER, W.G., 1977, Early Devonian flora of the Trout Valley Formation of northern Maine: Review of Palaeobotany and Palynology, v. 23, p. 255–285.

ANDREWS, H.N., KASPER, A., AND MENCHER, E., 1968, *Psilophyton forbesii*, a new Devonian plant from northern Maine: Bulletin of the Torrey Botanical Club, v. 95, p. 1–11.

BANKS, H.P., BONAMO, P.M., AND GRIERSON, J.D., 1972, *Leclercqia complexa* gen. et sp. nov., a new Lycopod from the late Middle Devonian of eastern New York: Review of Palaeobotany and Palynology, v. 14, p. 19–40, doi: 10.1016/0034-6667(72)90005-X.

Barthlott, W., Mail, M., Bhushan, B., and Koch, K., 2017, Plant surfaces: structures and functions for biomimetic innovations: Nano-Micro Letters, v. 9, p. 1–40.

Beck, C.B., 1962, Reconstructions of *Archaeopteris*, and further consideration of its phylogenetic position: American Journal of Botany, v. 49, p. 373–382.

Becker, R.T., Marshall, J.E.A., Da Silva, A.C., Agterberg, F.P., Gradstein, F.M., and Ogg, J.G., 2020, The Devonian period, *in* F.M. Gradstein, J.G. Ogg, M.D. Schmitz, and G.M. Ogg (eds.), Geologic Time Scale 2020: Elsevier, Amsterdam, p. 733–810.

Benca, J.P., Carlisle, M.H., Bergen, S., and Strömberg, C.A., 2014, Applying morphometrics to early land plant systematics: a new *Leclercqia* (Lycopsida) species from Washington State, USA: American Journal of Botany, v. 101, p. 510–520.

Berry, C.M. and Fairon-Demaret, M., 2001, The Middle Devonian flora revisited, in P.G. Gensel and D. Edwards (eds.), Plants Invade the Land: Evolutionary and Environmental Perspectives: Columbia University Press, New York, p. 120–139.

Berry, C.M. and Marshall, J.E.A., 2015, Lycopsid forests in the early Late Devonian paleoequatorial zone of Svalbard: Geology, v. 43, p. 1043–1046, doi: 10.1130/G37000.1.

Bond, W.J. and Keeley, J.E., 2005, Fire as a global 'herbivore': the ecology and evolution of flammable ecosystems: Trends in Ecology and Evolution, v. 20, p. 387–394.

Bonamo, P.M., Banks, H.P., and Grierson, J.D., 1988, *Leclercqia*, *Haskinsia*, and the role of leaves in delineation of Devonian lycopod genera: Botanical Gazette, v. 149, p. 222–239.

Boone, G.M., 1970, The Fish River Lake Formation and its environments of deposition: Maine Geological Survey Bulletin, v. 23, p. 27–41.

Bowman, D.M., Balch, J.K., Artaxo, P., Bond, W.J., Carlson, J.M., Cochrane, M.A., D'Antonio, C.M., Defries, R.S., Doyle, J.C., Harrison, S.P., and Johnston, F.H., 2009, Fire in the Earth system: Science, v. 324, p. 481–484.

Bradley, D. and Tucker, R., 2002, Emsian synorogenic paleogeography of the Maine Appalachians: The Journal of Geology, v. 110, p. 483–492.

Bradley, D.C., Tucker, R.D., Lux, D.R., Harris, A.G., and McGregor, D.C., 2000, Migration of the Acadian orogen and foreland basin across the northern Appalachians of Maine and adjacent areas: United States Geological Survey Professional Paper 1624, p. 1–49.

Capel, E., Cleal, C.J., Xue, J., Monnet, C., Servais, T., and Cascales-Miñana, B., 2022, The Silurian–Devonian terrestrial revolution: diversity patterns and sampling bias of the vascular plant macrofossil record: Earth-Science Reviews, v. 231, article 104085.

Chuvieco, E., Giglio, L., and Justice, C., 2008, Global characterization of fire activity: toward defining fire regimes from Earth observation data: Global Change Biology, v. 14, p. 1488–1502.

Crelling, J.C., Glasspool, I.J., Gibbins, J.R., and Seitz, M., 2005, Bireflectance imaging of coal and carbon specimens: International Journal of Coal Geology, v. 64, p. 204–216.

Davies, N.S., McMahon, W.J., and Berry, C.M., 2024, Earth's earliest forest: fossilized trees and vegetation-induced sedimentary structures from the Middle Devonian (Eifelian) Hangman Sandstone Formation, Somerset and Devon, SW England: Journal of the Geological Society, v. 181, article jgs2023–204, doi: 10.1144/jgs2023-204, open access.

Decombeix, A.L., Meyer-Berthaud, B., and Galtier, J., 2011, Transitional changes in arborescent lignophytes at the Devonian–Carboniferous boundary: Journal of the Geological Society, v. 168, p. 547–557.

Diessel, C.F., 2010, The stratigraphic distribution of inertinite: International Journal of Coal Geology, v. 81, p. 251–268.

Dorf, E. and Rankin, D.W., 1962, Early Devonian plants from the Traveler Mountain area, Maine: Journal of Paleontology, v. 36, p. 999–1004.

Edwards, D. and Axe, L., 2004, Anatomical evidence in the detection of the earliest wildfires: PALAIOS, v. 19, p. 113–128.

Edwards, D., Cherns, L., and Raven, J.A., 2015, Could land-based early photosynthesizing ecosystems have bioengineered the planet in mid-Palaeozoic times?: Palaeontology, v. 58, p. 803–837.

Fairon-Demaret, M., 1986, *Stockmansella*, a new name for *Stockmansia* Fairon-Demaret (Fossil): Taxon, v. 35, p. 334–334.

Gastaldo, R.A., 1994. The genesis and sedimentation of phytoclasts with examples from coastal environments, *in* A. Traverse (ed.) Sedimentation of Organic Particles: Cambridge University Press, Cambridge, p. 103–127.

Gastaldo, R.A., 2016, New paleontological insights into the Emsian–Eifelian Trout Valley Formation, Baxter State Park's Scientific Forest Management Area, Aroostook County, Maine: PALAIOS, v. 31, p. 339–346.

Gensel, P.G., 2018, Early Devonian woody plants and implications for the early evolution of vascular cambia, *in* N. Krings, C.J. Harper, N.R. Cúneo, and G.W. Rothwell (eds.), Transformative Paleobotany: Academic Press, Cambridge MA, p. 21–33, doi: 10.1016/B978-0-12-813012-4.00002-4.

Gensel, P.G. and Kasper, A.E., 2005, A new species of the Devonian lycopod genus, *Leclercqia*, from the Emsian of New Brunswick, Canada: Review of Palaeobotany and Palynology, v. 137, p. 105–123, doi: 10.1016/j.revpalbo.2005.08.005.

Gensel, P.G. and Albright, V.M., 2006, *Leclercqia complexa* from the Early Devonian (Emsian) of northern New Brunswick, Canada: Review of Palaeobotany and Palynology, v. 142, p. 103–121.

Gensel, P., Kasper, A., and Andrews, H.N., 1969, *Kaulangiophyton*, a new genus of plants from the Devonian of Maine: Bulletin of the Torrey Botanical Club, v. 96, p. 265–276.

Gensel, P., Glasspool, I., Gastaldo, R.A., Libertin, M., and Kvacke, J., 2020, Back to the beginnings: the Silurian–Devonian as a time of major innovation in plants and their communities, *in* E. Martinetto, E. Tschopp, and R.A. Gastaldo (eds.), Nature Through Time: Springer Nature Switzerland, Cham, Switzerland, p. 367–398, ISBN 978-3-030-35057-4.

Gerrienne, P., Meyer-Berthaud, B., Yang, N., Steemans, P., and Li, C.S., 2014, *Planatophyton* gen. nov., a late Early or Middle Devonian euphyllophyte from Xinjiang, North-West China: Review of Palaeobotany and Palynology, v. 208, p. 55–64.

Gerschel, H., Rascher, J., Volkmann, N., Ligouis, B., Kus, J., Bretschneider, F., and Schneider, W., 2018, Lignite oxidation under the influence of glacially derived groundwater: the pyropissite deposits of Zeitz-Weißenfels (Germany): International Journal of Coal Geology, v. 189, p. 50–67.

Giesen, P. and Berry, C.M., 2013, Reconstruction and growth of the early tree *Calamophyton* (Pseudosporochnales, Cladoxylopsida) based on exceptionally complete specimens from Lindlar, Germany (Mid-Devonian): organic connection of *Calamophyton* branches and *Duisbergia* trunks: International Journal of Plant Sciences, v. 174, p. 665–686.

Glasspool, I. and Scott, A.C., 2010, Phanerozoic concentrations of atmospheric oxygen reconstructed from sedimentary charcoal: Nature Geoscience, v. 3, p. 627–630, doi: 10.1038/ngeo923.

Glasspool, I.J. and Gastaldo, R.A., 2022a, Silurian wildfire proxies and atmospheric oxygen: Geology, v. 50, p. 1048–1052.

Glasspool, I.J. and Gastaldo, R.A., 2022b, A baptism by fire: fossil charcoal from eastern Euramerica reveals the earliest (Homerian) terrestrial biota evolved in a flammable world: Geological Society of London, article jgs2022-072, doi: 10.1144/jgs2022-072.

Glasspool, I.J., Scott, A.C., Waltham, D., Pronina, N., and Shao, L., 2015, The impact of fire on the late Paleozoic Earth system: Frontiers in Plant Science, v. 6, p. 756, doi: 10.3389/fpls.2015.00756.

Gribble, C.C. and Hall, A.J., 1992, Optical Mineralogy: Principles and Practice: UCL Press Ltd., London, 303 p.

Grierson, J.D. and Bonamo, P.M., 1979, *Leclercqia complexa*: earliest ligulate lycopod (Middle Devonian): American Journal of Botany, v. 66, p. 474–476.

Harrison, S.P., Bartlein, P.J., Brovkin, V., Houweling, S., Kloster, S., and Prentice, I.C., 2018, The biomass burning contribution to climate-carbon-cycle feedback: Earth System Dynamics, v. 9, p. 663–677.

Harrison, S.P., Prentice, I.C., Bloomfield, K.J., Dong, N., Forkel, M., Forrest, M., Ningthoujam, R.K., Pellegrini, A., Shen, Y., Baudena, M., and Cardoso, A.W., 2021, Understanding and modelling wildfire regimes: an ecological perspective: Environmental Research Letters, v. 16, article 125008.

Hueber, F.M. and Banks, H.P., 1967, *Psilophyton princeps*: the search for organic connection: Taxon, v. 16, p. 81–85.

ISO 7404-2, 2009, Methods for the Petrographic Analysis of Coals—Part 2: Methods of Preparing Coal Samples, 9 p.

ISO-7404-5:1994(E), 1994, Methods for the petrographic analysis of bituminous coal and anthracite: Part 5: Method of determining microscopically the reflectance of vitrinite: Geneva, International Organization for Standardization, 12 p.

Jones, M.W., Abatzoglou, J.T., Veraverbeke, S., Andela, N., Lasslop, G., Forkel, M., Smith, A.J., Burton, C., Betts, R.A., Van Der Werf, G.R., and Sitch, S., 2022, Global and regional trends and drivers of fire under climate change: Reviews of Geophysics, v. 60, article e2020RG000726.

Kasper, A.E. and Andrews, Jr., H.N., 1972, *Pertica*, a new genus of Devonian plants from northern Maine: American Journal of Botany, v. 59, p. 97–911.

Kasper, A.E. and Forbes, W.H., 1979, The Devonian lycopod *Leclercqia* from the Trout Valley Formation of Maine: Geological Society of Maine, Maine Geology Bulletin, v. 1, p. 49–59.

Kasper, A.E. and Forbes, W.H., 1983, An early occurrence of *Psilophyton* from the Upper Silurian/Lower Devonian Fish River Lake Formation in northern Maine: American Journal of Botany v. 70, p. 72.

Kasper, A.E., Andrews, H.N., and Forbes, W.H., 1974, New fertile species of *Psilophyton* from the Devonian of Maine: American Journal of Botany, v. 6, p. 339–359.

Kasper, Jr., A.E., Gensel, P.G., Forbes, W.H., and Andrews, Jr., H.N., 1988, Plant paleontology in the State of Maine: a review: Studies in Maine Geology, v. 1, p. 109–128.

Kennedy, K.L., Gensel, P.G., and Gibling, M.R., 2012, Paleoenvironmental inferences from the classic Lower Devonian plant-bearing locality of the Campbellton Formation, New Brunswick, Canada: PALAIOS, v. 27, p. 424–438.

Kenrick, P. and Crane, P.R., 1997, The origin and early evolution of plants on land: Nature, v. 389, p. 33–39.

Lasslop, G., Coppola, A.I., Voulgarakis, A., Yue, C., and Veraverbeke, S., 2019, Influence of fire on the carbon cycle and climate: Current Climate Change Reports, v. 5, p. 112–123.

Lu, M., Ikejiri, T., and Lu, Y., 2021, A synthesis of the Devonian wildfire record: implications for paleogeography, fossil flora, and paleoclimate: Palaeogeography, Palaeoclimatology, Palaeoecology, v. 571, article 110321.

Malinconico, M.A., 2023, Very-low-grade metamorphic trends in the Aroostook-Matapedia belt of northeastern Maine using graptolite and vitrinite reflectance, and other indicators: New England Intercollegiate Geological Conference 2023, University of Maine, Presque Isle, p. 1–9.

Malinconico, M.A.L., 1993a, Reflectance cross-plot analysis of graptolites from the anchi-metamorphic region of northern Maine, USA: Organic Geochemistry, v. 20, p. 197–207.

Malinconico, M.L., 1993b, Preliminary vitrinite reflectance study of the post-Acadian Mapleton and Trout Valley Formation, northern Maine: Geological Society of America, Abstracts with Programs, v. 25, n. 2, annual GSA Northeastern Section meeting, Burlington, Vermont, 22–24 March 1993, ISSN 0016-7592.

Marshall, J.E., Holterhoff, P.F., El-Abdallah, S.R., Matsunaga, K.K., Bronson, A.W., and Tomescu, A.M., 2022, The archaeopterid forests of lower Frasnian (Upper Devonian) westernmost Laurentia: biota and depositional environment of the Maywood Formation in Northern Wyoming as reflected by palynoflora, macroflora, fauna, and sedimentology: International Journal of Plant Sciences, v. 183, p. 465–492.

Mastalerz, M., Hampton, L., and Drobniak, A., 2016, Evaluating thermal maturity using transmitted light techniques: color changes in structureless organic matter and palynomorphs: Indiana Geological Survey Occasional Paper, v. 73, p. 1–41.

McGregor, D.C., 1977, Lower and Middle Devonian spores of eastern Gaspé, Canada, II, Biostratigraphy: Palaeontographica Abteilung B, v. 163, p. 111–142.

McGregor, D.C., 1992, Palynomorph evidence for the age of the Trout Valley Formation of northern Maine: Geological Survey of Canada, Report F1-9-1992, 4 p.

McGregor, D.C. and Camfield, M., 1976, Upper Silurian (?) to Middle Devonian spores of the Moose River Basin, Ontario: Geological Survey of Canada Bulletin, v. 263, p. 1–63.

Meyer-Berthaud, B., Fairon-Demaret, M., Steemans, P., Talent, J., and Gerrienne, P., 2003, The plant *Leclercqia* (Lycopsida) in Gondwana: implications for reconstructing Middle Devonian palaeogeography: Geological Magazine, v. 140, p. 119–130, doi: 10.1017/S0016756802007276.

Meyer-Berthaud, B., Soria, A., and Decombeix, A.L., 2010, The land plant cover in the Devonian: a reassessment of the evolution of the tree habit: Geological Society, London, Special Publications, v. 339, p. 59–70.

Mills, B.J., Krause, A.J., Jarvis, I., and Cramer, B.D., 2023, Evolution of atmospheric O_2 through the Phanerozoic, revisited: Annual Review of Earth and Planetary Sciences, v. 51, p. 253–276, doi: 10.1146/annurev-earth-032320-095425.

Mousa, D.A., Makled, W.A., Gentzis, T., Gad, N.S., and Samaan, J., 2022, Discovery of an extraordinary Carboniferous cutinite-rich coal seam from Wadi Abu Thora, southern Sinai, Egypt: organic petrographical and geochemical characterization: International Journal of Coal Geology, v. 250, article 103908.

Nichols, G. and Jones, T., 1992, Fusain in Carboniferous shallow marine sediments, Donegal, Ireland: the sedimentological effects of wildfire: Sedimentology, v. 39, p. 487–502.

Pausas, J.G. and Keeley, J.E., 2009, A burning story: the role of fire in the history of life: BioScience, v. 59, p. 593–601.

Pausas, J.G., Keeley, J.E., and Schwilk, D.W., 2017, Flammability as an ecological and evolutionary driver: Journal of Ecology, v. 105, p. 289–297.

Pearson, T. and Scott, A.C., 1999, Large palynomorphs and debris, in T.P. Jones and N.P. Rowe (eds.), Fossil Plants and Spores: Modern Techniques: Geological Society, London, p. 20–25.

Pfeiler, K.C., Tomescu, A.M.F., and Seyfullah, L., 2021, An Early Devonian actinostelic euphyllophyte with secondary growth from the Emsian of Gaspé (Canada) and the importance of tracheid wall thickening patterns in early euphyllophyte systematics: Papers in Palaeontology, v. 7, p. 1081–1095, doi: 10.1002/spp2.1335.

Potonié, H., 1910, Kaustobiolithe: Geologische Rundschau, v. 1, p. 327–337.

Pšenička, J., Bek, J., Frýda, J., Žárský, V., Uhlířová, M., and Štorch, P., 2021, Dynamics of Silurian Plants as Response to Climate Changes: Life 2021, v. 11, p. 906, doi: 10.3390/life11090906.

Richardson, J.B., and McGregor, D.C., 1986, Silurian and Devonian spore zones of the Old Red Sandstone region: Geological Survey of Canada Bulletin, v. 364, p. 1–79.

Schopf, J.M., 1964, Middle Devonian plant fossils from northern Maine: United States Geological Survey Professional Paper, v. 501, p. D43–D49.

Schopf, J.M., Mencher, E., Boucot, A.J., and Andrews, H.N., 1966, Erect plants in the early Silurian of Maine: United States Geological Survey Professional Paper, v. 550, p. D69–D75.

Scotese, C.R. and McKerrow, W.S., 1990, Revised world maps and introduction: Geological Society, London, Memoirs, v. 12, p. 1–21.

Scotese, C.R., Song, H., Mills, B.J., and Van Der Meer, D.G., 2021, Phanerozoic paleotemperatures: the Earth's changing climate during the last 540 million years: Earth-Science Reviews, v. 215, article 103503.

Scott, A.C., 2010, Charcoal recognition, taphonomy and uses in palaeoenvironmental analysis: Palaeogeography, Palaeoclimatology, Palaeoecology, v. 291, p. 11–39.

Scott, A.C. and Glasspool, I.J., 2006, The diversification of Paleozoic fire systems and fluctuations in atmospheric oxygen concentration: Proceedings of the National Academy of Sciences, v. 103, p. 10861–10865.

Scott, A.C. and Glasspool, I.J., 2007 Observations and experiments on the origin and formation of inertinite group macerals: International Journal of Coal Geology, v. 70, p. 53–66.

Selover, R.W., Gastaldo, R.A., and Nelson, R.E., 2005, An estuarine assemblage from the Middle Devonian Trout Valley Formation of northern Maine: PALAIOS, v. 20, p. 192–197.

Song, D.F., Wang, T.G., Li, P., Zhang, M., Liu, A.L., and Yan, J.D., 2022, Petrology and organic geochemistry of the Baishaping and Damaidi Devonian cutinitic liptobioliths, west of the Kangdian Uplift, China: Petroleum Science, v. 19, p. 1978–1992.

Stach, E., Mackowsky, M.T., Teichmüller, M., Taylor, G.H., Chandra, D., and Teichmüller, R., 1982, Stach's textbook of coal petrology: Gebrüder Borntraeger, Berlin, 535 p.

Stein, W.E., Mannolini, F., Hernick, L.V., Landing, E., and Berry, C., 2007, Giant cladoxylopsid trees resolve the enigma of the Earth's earliest forest stumps at Gilboa: Nature, v. 446, p. 904–907.

Stein, W.E., Berry, C.M., Hernick, L.V., and Mannolini, F., 2012, Surprisingly complex community discovered in the mid-Devonian fossil forest at Gilboa: Nature, v. 483, p. 78–81.

Stein, W.E., Berry, C.M., Morris, J.L., Hernick, L.V., Mannolini, F., Ver Straeten, C., Landing, E., Marshall, J.E., Wellman, C.H., Beerling, D.J., and Leake, J.R., 2020, Mid-Devonian *Archaeopteris* roots signal revolutionary change in earliest fossil forests: Current Biology, v. 30, p. 421–431.

Strother, P.K. and Lenk, C., 1983, *Eohostimella* is not a plant: American Journal of Botany, v. 70, p. 80, abstract only.

Strullu-Derrien, C., Servais, T., and Kenrick, P., 2023, Insights into palaeobotany: Botany Letters, v. 170, p. 157–164.

Sturm, H., 2009, Archaeognatha: (Bristletails), *in* V.H. Resh and R.T. Cardé (eds.), Encyclopedia of Insects: Academic Press, Cambridge, MA, p. 48–50.

Teichmüller, M., Teichmüller, R., and Bartenstein, H., 1979, Inkohlung und Erdgas in Nordwestdeutschland. Eine Inkohlungskarte der oberfläche des oberkarbons: Fortschritte in der Geologie von Rheinland und Westfalen, v. 27, p. 137–170.

Van Der Werf, G.R., Randerson, J.T., Giglio, L., Van Leeuwen, T.T., Chen, Y., Rogers, B. M., Mu, M., Van Marle, M.J., Morton, D.C., Collatz, G.J., and Yokelson, R.J., 2017, Global fire emissions estimates during 1997–2016: Earth System Science Data, v. 9, p. 697–720.

Vaughan, A. and Nichols, G., 1995, Controls on the deposition of charcoal; implications for sedimentary accumulations of fusain: Journal of Sedimentary Research, v. 65. p. 129–135, doi: 10.1306/D426804A-2B26-11D7-8648000102C1865D.

Wang, C., 2022, Bedrock geology of the Fish River Lake quadrangle, Maine: Maine Geological Survey, Geologic Map 22-5, scale 1:24,000.

Wang, C., Marvinney, R.G., Putnam, D., Bagley, E., and Belair, S., 2020, The newly discovered, giant Fish River post-Acadian rift system in the northern Appalachians of Maine: Geological Society of America Abstracts with Programs, v. 52, n. 6, p. 133.

Xue J.Z., Hao, S.G., Zhu, X, and Wang, D.M., 2012, A new basal euphyllophyte, *Pauthecophyton* gen. nov., from the Lower Devonian (Pragian) of Yunnan, China: Review of Palaeobotany and Palynology, v. 183, p. 9–20.

Xu, H.-E., Wang, Y., Chen, Y.-S., Huang, P., Zhang, X.-L., Wang, Y., Qiao, L, and Lu, J.-F., 2020, Spatio-temporal distribution of *Leclercqia* (Lycopsida), with its new discovery from the Middle to Upper Devonian of Yunnan, South China: Palaeogeography, Palaeoclimatology, Palaeoecology, v. 560, article 110029, doi: 10.1016/j.palaeo.2020.110029.

Yue, C., Ciais, P., Zhu, D., Wang, T., Peng, S.S., and Piao, S.L., 2016, How have past fire disturbances contributed to the current carbon balance of boreal ecosystems?: Biogeosciences, v. 13, p. 675–690.

Received 15 April 2024; accepted 2 July 2024.